TWO-PHOTON EXCHANGE CORRECTIONS AT LARGE MOMENTUM TRANSFER REVISED*

Nikolay Kivel [ORCID]

Physik Department, Technische Universität München [ROR]
James-Franck-Str. 1, 85748 Garching, Germany

Motivated by experimental data at large momentum transfer, we update the analysis of the two-photon exchange effect in the electron–nucleon scattering using the effective field theory formalism. Our approach is suitable for describing the hard $s \sim |t| \sim |u| \gg \Lambda^2$ region, where the hadronic model calculations are not accurate enough. We improve the estimates of various long-range matrix elements and discuss the obtained numerical effects for the unpolarised elastic cross section. Assuming a linear behaviour of the reduced cross section with respect to the photon polarisation, we show that the obtained description allows us to resolve the form factor discrepancy for $Q^2 = 2.5$–3.5 GeV^2. However, the effect obtained is quite small for higher values of Q^2. It is possible that nonlinear effects may be important in understanding the discrepancy in this region. Estimates of the elastic electron–neutron cross section in the region of $Q^2 = 2.5$–3.5 GeV^2 are also performed. The obtained TPE effects are sufficiently large and must be taken into account.

Dedicated to Mitya, Vitya, and Maxim

I first met Maxim back at the Saint Petersburg University, apparently in 1989. The Faculty of Physics and the Institute of Physics were located in Peterhof, a suburb of Saint Petersburg, and we both lived on campus there, in the student dormitories.

Maxim was already a senior student and participated as an equal in scientific discussions with the department staff. I was just starting my fifth semester, so I could only attend as a listener, as I did not yet understand anything in those discussions. Terms like 'pions', 'K-mesons', and 'SU(3) violation' were completely unclear to me. This strongly motivated me to pursue self-education, developing independently of the basic curriculum. At that time, Maxim was writing his diploma thesis at the Petersburg Institute

---

of Nuclear Physics under the supervision of two individuals unknown to me then, Mitya and Vitya. This was how I first became indirectly acquainted with D.I. Dyakonov (Mitya) and V.Yu. Petrov (Vitya).

Later, I joined the group of Prof. A.N. Vasiliev, who worked on quantum field theory and its applications in statistical physics. After defending my diploma at the end of 1992, I entered the Ph.D. program in the theoretical department of PNPI. At that time, I was eager to switch to interesting problems in elementary particle physics.

One of the opportunities to better understand the research topics of the theoretical department and get to know its members was the in-house theoretical seminar. It was during these seminars that I first met Mitya and Vitya in person. These seminars were not the typical 45-minute sessions common almost everywhere today. They were held every Monday and could last up to four hours with a short break. This seminar was a characteristic feature of the theoretical department, and it seems the tradition originated with V. Gribov, who inherited it from the seminars of Academician Lev Landau. During the speaker's presentation, it was normal to constantly ask questions, critique, demand additional explanations, disagree with certain points by explaining the reasoning to everyone, or, conversely, provide alternative explanations and diverse commentary. Often, complex debates arose among participants that sometimes became unclear even to the speaker. Overall, it was a lively forum — a place for discussion where the speaker faced extensive criticism, sometimes constructive, sometimes not, and had to clearly explain and defend his methods and conclusions while considering various perspectives and approaches from the audience.

Undoubtedly, the most active participants, including Vitya and Mitya, formed the core of this forum. Speakers often received the most questions and criticism from Vitya, who sometimes reacted passionately to claims or hypotheses he deemed incorrect. 'But Landau and Lifshitz already wrote about this in the third volume (Quantum Mechanics)!' he would often exclaim. Mitya was not far behind, though he spoke more calmly, usually presenting very strong arguments. To convince them, a speaker not only needed a deep understanding of the topic but also had to be able to clearly explain where Mitya and Vitya might be mistaken.

It took me considerable time to properly grasp the terminology and the commonly used working jargon, and even after that, I still felt uncertain for a long time. Somehow, it so happened that I found myself without a scientific advisor for an extended period of time. By that time, many good researchers had already left to work in various laboratories abroad, and finding a topic that would interest and captivate me turned out to be difficult. Thus, I continued working on my diploma thesis topic with the university group,focusing more on mathematical issues in statistical models of quantum field theory.

In the fall of 1993, after one of the seminars, Mitya approached me: 'We have a tradition', he said. 'We assign young Ph.D. students an overview talk on a completely new and unfamiliar topic they have not worked on before. So we've decided to ask you to prepare a talk on the heavy-quark effective theory. This topic is very popular now, and it will be very useful for everyone to learn more about it.'

I must admit, this hit the mark precisely — I knew absolutely nothing about the physics or phenomenology of heavy quarks! Moreover, at that time, I had not yet published anything at all on elementary particle physics. For this reason, the complexity of the task sounded to me almost like the famous phrase from a Russian fairy tale: 'Go there, I don't know where, bring that, I don't know what.' I felt uneasy. 'Could you recommend anything for reading and preparation?' I asked Mitya. 'Talk to Kolya Uraltsev; he's just back for a short while and will be in the theoretical department on Thursday.'

That did not make me feel much better. I had only heard of Kolya but had not met him personally, as he was almost always away working abroad. I managed to meet Kolya at the institute only once. He was very busy with some administrative matters, quickly handed me two preprints without much explanation, and rushed off. That was the entirety of our interaction. The preprints turned out to be original articles on B-meson decays, intended for an advanced reader, and I found almost nothing useful in them for myself. Even the first formula for the effective heavy-quark field was unclear to me — its derivation and reasoning were not provided in detail.

Tracing references in those papers also yielded no results, as they were similar original works intended for advanced readers. Ultimately, it seemed I would need to independently derive nearly all the fundamentals of the effective theory, which was, of course, unrealistic. I became despondent, as I could not find a reasonable way to prepare for the talk.

Another psychological factor added to the pressure. Mitya was known for his plain dealing in evaluations. He sincerely believed that if someone, in his opinion, is not suitable for research work, then it is better to tell him about it directly. Usually, this sounded like a recommendation not to engage in science. Given Mitya's authority, such a recommendation was not easy to hear. I personally witnessed one such conversation with a student who had incorrectly solved a problem during the theoretical minimum exam to enter the Ph.D. program in the theoretical department. Since Mitya had personally assigned me the task, I feared that if I did not prepare adequately, I would face a similar fate.

Fortunately, the situation with the talk was eventually resolved. I cannot remember how, but I found a reference to a recently published review by Neubert titled *Heavy-quark symmetry*, available in the electronic `hep arXiv` [1]. It was exactly what I needed — a superb introduction to the

physics of heavy quarks and specifically HQET, which I had to present to the seminar audience. With this discovery, my stressful struggle ended, and the preparation became genuinely enjoyable. I delved deeply into the physics and technical details, reproduced some calculations myself, and successfully prepared and delivered the seminar. This was essentially my first experience of independently mastering a completely new and unfamiliar topic, which gave me confidence and provided knowledge that proved valuable later.

Several years later, while in Germany, I more than once met with Mitya and Vitya in Bochum, where I was working at the time in Prof. Klaus Goeke's group. They were actively collaborating with Klaus and Maxim on various topics, such as pentaquarks and various applications of the quark-soliton model. One day, I mentioned to Vitya that there was still a lack of data on hard exclusive processes. He disagreed, arguing that, in his view, the available data were sufficient, but that the major gap is in the theory — we do not understand confinement and cannot systematically calculate all necessary quantities in QCD from first principles. He and Mitya were actively working on the understanding of the confinement in QCD, and Vitya firmly believed that it was purely a theoretical challenge. To me, it seemed strange that such a fundamental issue could exist independently of experiments, but on the other hand, I could not propose a way to experimentally study confinement either. However, I believed that our lack of understanding of low-energy dynamics might be due to insufficient data that could guide us to the right solution, so experimental exploration is also crucial. From this point of view, hard exclusive processes are especially interesting because they involve a combination of QCD dynamics at small and large distances and provide access to a new information. We started a discussion, but of course I could not convince Vitya.

Despite this somewhat skeptical point of view, Vitya in collaboration with Maxim produced a number of interesting works on calculating hadron wave functions (or, more precisely, light-cone distribution amplitudes, LCDAs) in the quark-soliton model. These functions are very important for the description of various exclusive reactions. One of their papers focused on nucleon LCDAs and the calculation of the proton's electromagnetic form factors. For reasons unknown to me, these results were only published as an electronic preprint. Several years later, I needed different models for nucleon LCDAs for my work, but I could not find the parameterisation I required in their paper. I approached Maxim, explaining that there were significantly different estimates of an important constant obtained through QCD sum rules and lattice calculations. Therefore, it would be very interesting to see what value this constant could have in the quark-soliton model. Maxim promised to calculate the constant, and just a few days before his tragic passing, he told me that the preliminary result was ready, needing only verification and evolution to the relevant scale for comparison with other results. This work was later completed and published by his colleagues.

In terms of scientific collaboration, my closest interaction is with Maxim. Most of our joint works, with rare exceptions, were related to the study of Generalised Parton Distributions (GPDs) and understanding of Deeply Virtual Compton Scattering. While I was primarily interested in the factorisation process and the calculation of radiative and power corrections, Maxim was more focused on the properties of non-perturbative matrix elements. In this way, we complemented and learned from each other. It was thanks to him that I became interested in chiral perturbation theory and its application to the description of non-perturbative functions in hard processes. One of the first ideas of this kind was the study of pion GPDs and soft-pion low-energy theorems for these functions. Specifically, the chiral calculation automatically provided the correct structure of the double distribution for GPDs, including the so-called D-term, which, for example, is absent in the naive model associated with the triangle diagram.

When we started this project, I was completely unfamiliar with chiral perturbation theory, so I had to draw on my prior experience studying HQET, as described earlier. I found several reviews, studied them thoroughly, and quickly joined the work. This experience enriched my understanding of the effective field theory approach and proved valuable for other applications later.

Further study of chiral loop corrections led us to conclude that the chiral expansion for GPDs breaks down in the region of small Bjorken $x_{\rm Bj}$. The resulting problem, in principle, could only be resolved by resumming all orders of the chiral expansion. At first glance, this task seemed insurmountable, but we quickly realised it could be significantly simplified by assuming that the dominant contribution came from leading chiral logarithms. In this case, it turned out that the pion could be treated as massless, and we could focus only on four-particle vertices with derivatives in the full chiral Lagrangian. Essentially, the problem reduced to one-loop renormalisation of an infinite number of effective constants in this effective action. However, even in this case, renormalisation of the vertices remained complex and confusing due to their strong mixing with one another. Here, the experience I gained while studying critical statics proved helpful. The idea emerged to introduce a conformal basis for vertex operators, which greatly simplified the mixing structure, allowing us to derive a relatively simple recurrence relation for the coefficients of the large leading logarithms. I must say that working on this problem gave me immense satisfaction from solving mathematical challenges. It was especially paradoxical for me to see the problem reduced to conformal field theory. After all, at first glance, it was difficult to imagine that there could be any connection between conformal symmetry and chiral perturbation theory! Maxim was also fascinated, primarily by the mathematical aspects of our approach. Unfortunately, it turned out that from a practical standpoint, the effect of logarithm resummation was relatively small, though it provided some qualitative insight into the behaviour of the

chiral pion cloud in the small x_{Bj} region. Later, I became interested in calculating the two-photon contribution to elastic scattering and paused further work on this project. However, the experience gained in calculating chiral corrections and, more broadly, the perspective on the concept of low-energy effective theories became an integral part of my practical toolkit and proved extremely useful for solving some problems later, for which I am sincerely grateful to Maxim.

1. Introduction

The two-photon exchange (TPE) contribution gives us the most plausible explanation of the discrepancy in the extraction of the proton ratio $G_{\mathrm{E}}/G_{\mathrm{M}}$ using the Rosenbluth (or LT separation) and the polarisation transfer methods, see *e.g.* reviews [2–6]. Many different TPE calculations have been carried out in the region of $Q^2 < 5$ GeV^2. This includes the various hadronic model calculations [7–10] and also the dispersive framework [11–16]. These estimates allow one to obtain the TPE contribution at relatively low $Q^2 \leq 2$ GeV^2. However, such calculations become less accurate in the region of higher values of the momentum transfer, since they do not properly take into account the effects of short-range dynamics. This becomes especially important in the region where all Mandelstam variables describing the *ep*-scattering are large

$$s \sim -t \sim -u \gg \Lambda^2 \,, \tag{1}$$

where Λ is the typical hadronic scale. For any large Q^2, there is the region $\varepsilon > \varepsilon_{\mathrm{min}}$ where condition (1) is satisfied. In this region, the calculations of the hadron model have a large uncertainty from the contribution of excited states. With the growth of Q^2, the value of $\varepsilon_{\mathrm{min}}$ decreases, limiting more and more the applicability domain of the hadron model.

Polarisation measurements of $\mu_p G_{\mathrm{E}}/G_{\mathrm{M}}$ show that this ratio decreases monotonically with increasing Q^2 and becomes quite small in the region of $Q^2 \sim 9$–10 GeV^2. At the same time, the LT separation approach suggests that this ratio remains large $\mu_p G_{\mathrm{E}}/G_{\mathrm{M}} \sim 1$–2 [17, 18]. This discrepancy could be interpreted as the TPE correction being large and dominant in this kinematic region. A description of the TPE amplitudes, in this case, must include the effects from the short- and long-distance dynamics in a systematic way.

The collinear factorisation of TPE amplitudes at large momentum transfer was considered in Refs. [19, 20]. Such a description includes only the hard-spectator mechanism. The experience in the description of proton FFs allows one to expect that the soft-spectator contributions are also large [21–23] and therefore they can also provide sufficiently large numerical effect. The first attempt to consider such a mechanism was done in Ref. [24] using the GPD-model framework. A more systematic treatment based on the effective field theory (EFT) framework was considered in Ref. [25].

In the EFT approach, the soft-spectator contribution is described in terms of appropriate soft-collinear matrix elements associated with the soft and collinear particles. Corresponding momenta are of the order of $p_{\rm s}^2 \sim \Lambda^2$ and $p_{\rm hc}^2 \sim \Lambda Q$ for the soft- and hard-collinear particles, respectively. These contributions are considered as non-perturbative. The hard interactions associated with the momenta $p_{\rm h}^2 \sim Q^2$ are computed using the perturbative QCD (pQCD). Such an approach allows one to include hard- and soft-spectator contributions in a systematic way.

In the current work, we update the numerical calculations carried out in Ref. [25] for the reduced cross section. We are also going to clarify some uncertainties associated with long-distance matrix elements. The TPE effect in the cross section with a neutron target is also discussed.

The paper is organised as follows. In Section 2, we discuss the analytical structure of the TPE amplitudes, briefly review the results obtained previously for these amplitudes, and provide an explicit formula for the unpolarised cross section used in the phenomenological analysis. In Section 3, we carry out the phenomenological analysis of the existing data for the elastic electron–proton scattering. Section 4 is devoted to the TPE calculations for the elastic electron–neutron scattering. In Section 5, we briefly discuss the obtained results and conclusions. In three appendices, we provide some important technical details.

2. The TPE contribution within the EFT framework

In this paper, we use the same notation as in Ref. [25]. For simplicity, we will consider the description of a proton target. Specific features of a neutron target will be discussed later.

The expression for the TPE amplitude is given by

$$A_{ep}^{\gamma\gamma} = \frac{e^2}{Q^2} \bar{u}\left(k'\right) \gamma_\mu u(k) \ \bar{N}\left(p'\right) \ \hat{T}^\mu \left(\varepsilon, Q^2\right) \ N(p) \,, \tag{2}$$

where $\bar{u}(k'), u(k)$ and $\bar{N}(p'), N(p)$ denote lepton and nucleon spinors, respectively. The amplitude $\hat{T}^\mu$ reads [27]

$$\hat{T}^\mu \left(\varepsilon, Q^2\right) = \gamma^\mu \delta \tilde{G}_{\rm M}^{2\gamma} \left(\varepsilon, Q^2\right) - \frac{P^\mu}{m} \delta \tilde{F}_2 \left(\varepsilon, Q^2\right) + \frac{P^\mu}{m^2} \slashed{K} \ \tilde{F}_3 \left(\varepsilon, Q^2\right) \,, \tag{3}$$

where

$$P = \frac{1}{2}\left(p + p'\right) \,, \qquad K = \frac{1}{2}\left(k + k'\right) \,, \tag{4}$$

and m denotes the nucleon mass. Variables ε and Q^2 denote the photon polarisation and momentum transfer as usual. The reduced elastic cross

section is given by

$$
\sigma_{\mathrm{R}}^{\mathrm{el}}(\varepsilon, Q) \;=\; G_{\mathrm{M}}^2 + \frac{\varepsilon}{\tau} G_{\mathrm{E}}^2 + 2 G_{\mathrm{M}} \operatorname{Re}\left[\delta \tilde{G}_{\mathrm{M}}^{2\gamma} + \varepsilon \frac{\nu}{m^2} \tilde{F}_3\right]
$$
$$
+ 2\frac{\varepsilon}{\tau} G_{\mathrm{E}} \operatorname{Re}\left[\delta \tilde{G}_{\mathrm{E}} + \frac{\nu}{m^2} \tilde{F}_3\right], \tag{5}
$$

where $\tau = Q^2/4m$, $\nu = (K \cdot P)$, G_{M} and G_{E} are magnetic and electric form factors (FFs), respectively. Following the arguments discussed in Ref. [25], we neglect the second term on the r.h.s. of Eq. (5), assuming that the numerical effect of this term is sufficiently small due to the small G_{E}

$$
G_{\mathrm{M}} \operatorname{Re}\left[\delta \tilde{G}_{\mathrm{M}}^{2\gamma} + \varepsilon \frac{\nu}{m^2} \tilde{F}_3\right] \gg \frac{\varepsilon}{\tau} G_{\mathrm{E}} \operatorname{Re}\left[\delta \tilde{G}_{\mathrm{E}} + \frac{\nu}{m^2} \tilde{F}_3\right] \sim O(\alpha G_{\mathrm{E}}). \tag{6}
$$

Therefore, with very good accuracy, the reduced cross section is determined by the expression

$$
\sigma_{\mathrm{R}}^{\mathrm{el}}(\varepsilon, Q) \;\simeq\; G_{\mathrm{M}}^2\left(Q^2\right) + \frac{\varepsilon}{\tau} G_{\mathrm{E}}^2\left(Q^2\right)
$$
$$
+ 2 G_{\mathrm{M}}\left(Q^2\right) \operatorname{Re}\left[\delta \tilde{G}_{\mathrm{M}}^{2\gamma}(\varepsilon, Q) + \varepsilon \frac{\nu}{m^2} \tilde{F}_3(\varepsilon, Q)\right]. \tag{7}
$$

The interference term in the r.h.s. of Eq. (7) is proportional to the small electromagnetic coupling α, but for large values of Q^2 (large τ) this contribution can have a strong influence on the extraction of the small FF G_{E}^2.

In the forward limit, when $\varepsilon \to 1$ and Q^2 is fixed[1], the TPE correction vanishes

$$
\operatorname{Re}\left[\delta \tilde{G}_{\mathrm{M}}^{2\gamma}(\varepsilon, Q) + \varepsilon \frac{\nu}{m^2} \tilde{F}_3(\varepsilon, Q)\right]\bigg|_{\varepsilon \to 1} = 0, \tag{8}
$$

as it follows from the dispersion relations derived in Ref. [11].

In the kinematic region, where all Mandelstam variables are large $s \sim -t \sim -u \gg \Lambda^2$, the complex dynamics of QCD is sensitive to different scales associated with different scattering mechanisms. The amplitudes are given by the sum of the soft- and hard-spectator scattering contributions, which are designated by (s) and (h) superscripts, respectively

$$
\delta \tilde{G}_{\mathrm{M}}^{2\gamma}(\varepsilon, Q) \;=\; \delta \tilde{G}_{\mathrm{M}}^{(s)}(\varepsilon, Q) + \delta \tilde{G}_{\mathrm{M}}^{(h)}(\varepsilon, Q), \tag{9}
$$
$$
\tilde{F}_3(\varepsilon, Q) \;=\; \tilde{F}_3^{(s)}(\varepsilon, Q) + \tilde{F}_3^{(h)}(\varepsilon, Q). \tag{10}
$$

The hard-spectator contributions can be calculated using the QCD collinear factorisation approach [19, 20]. The analytical results are collected in Appendix A.

---

[1] This is equivalent in Mandelstam variables to the limit $s \to \infty$ and $-t$ is fixed.

The soft-spectator contributions are described by the product of the hard coefficient functions and long-distance matrix elements. The hard subprocess is associated with lepton–quark subprocess $eq \to eq$. In this case, both photons couple to a single active quark giving the box diagrams as in Fig. 1. It is assumed that the virtual photons and quark in this diagram have large virtualities of the order of Q^2.
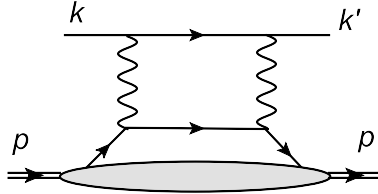

Fig. 1. The soft-spectator contribution. The grey blob denotes FF $\mathcal{F}_1(Q^2)$.

Therefore, the soft-spectator contribution $\tilde{F}_3^{(s)}$ can be represented as

$$\frac{\nu}{m^2} \tilde{F}_3^{(s)} \left(\varepsilon, Q^2\right) = \frac{\alpha}{\pi} \frac{\nu}{s} C_3 \left(\varepsilon, Q^2\right) \mathcal{F}_1 \left(Q^2\right) , \tag{11}$$

where $C_3(\varepsilon, Q^2)$ is the hard coefficient function describing the hard lepton–quark subprocess $eq \to eq$. The non-pertubative FF $\mathcal{F}_1(Q^2)$ describes the hard-collinear matrix element and includes the interactions of the soft- and hard-collinear modes in the EFT. This function can be restricted from the data for wide-angle Compton scattering (WACS) [25, 26].

The expression for $\delta \tilde{G}_{\mathrm{M}}^{(s)}$ includes two different contributions. One term describes a configuration in which both the photons and the loop quark are hard, as noted earlier. The second term is associated with the region, where photons have different virtualities: hard $q_1^2 \sim Q^2$ and soft $q_2^2 \sim \Lambda^2$ or *vice versa*. Therefore, the factorised expression reads

$$\delta \tilde{G}_{\mathrm{M}}^{(s)} \left(\varepsilon, Q^2\right) = \frac{\alpha}{\pi} C_{\mathrm{M}} \left(\varepsilon, Q^2, \mu_{\mathrm{F}}\right) \mathcal{F}_1 \left(Q^2\right) + \frac{\alpha}{\pi} g_1(\varepsilon, Q^2, \mu_{\mathrm{F}}). \tag{12}$$

Here, the hard-loop contribution is associated with the $C_{\mathrm{M}} \mathcal{F}_1$ term and C_{M} is the hard coefficient function, which can be found in Appendix B.

The amplitude g_1 describes the contributions with the soft photon. The hard–hard and hard–soft photon configurations overlap and the factorisation scale μ_{F} separates corresponding domains. It can be associated with the maximal virtuality of the soft photon.

The long-distance amplitude g_1 is defined by the matrix element in the EFT after factorisation of the hard subprocess. It is important to notice that this amplitude includes the infrared QED logarithm, which arises from

the TPE diagrams. In Ref. [25], the elastic contribution to g_1 is computed using the effective hadronic model. The result reads

$$g_1(\varepsilon, Q, \mu_{\mathrm{F}}) \simeq G_{\mathrm{M}}(Q^2) \ln \frac{\lambda^2}{\mu_{\mathrm{F}}^2} \ln \left| \frac{s - m^2}{u - m^2} \right| + g_{1\mathrm{R}}(\varepsilon, Q) \,, \tag{13}$$

where λ^2 is the photon mass used as an IR-regulator, s and u are the Mandelstam variables, which can be rewritten in terms of ε and Q^2 (recall, m is nucleon mass). The function $g_{1\mathrm{R}}$ in Eq. (13) includes inelastic IR-finite contributions. Such contributions are not considered in Ref. [25]. It turns out that at large Q^2 such contributions are suppressed and, therefore,

$$g_{1\mathrm{R}}(\varepsilon, Q, \mu_{\mathrm{F}}) \approx 0 \,. \tag{14}$$

A more detailed discussion of this point is provided in Appendix B. Therefore, the elastic approximation in Eq. (13) practically gives the dominant numerical effect in this case.

In order to compare our calculations with the experimental data, which have been corrected according to Mo and Tsai (MT) [28], we need to consider the following expression [25]:

$$\sigma_{\mathrm{R}}^{1\gamma,\mathrm{MT}} = \sigma_{\mathrm{R}}^{1\gamma} \left(1 + \delta_{2\gamma} - \delta_{2\gamma}^{\mathrm{MT}} \right) \,, \tag{15}$$

where $\sigma_{\mathrm{R}}^{1\gamma,\mathrm{MT}}$ is the reduced cross section obtained using MT radiative corrections, $\delta_{2\gamma}$ denotes the TPE correction obtained in the EFT framework, $\delta_{2\gamma}^{\mathrm{MT}}$ is the expression obtained in Ref. [28]. The analytical expression for the factor $\delta_{2\gamma}^{\mathrm{MT}}$ reads

$$\mathrm{Re}\, \delta_{2\gamma}^{\mathrm{MT}} \left(\varepsilon, Q^2 \right) = \frac{2\alpha}{\pi} \ln \frac{\lambda^2}{\tilde{s}} \ln \left| \frac{\tilde{s}}{\tilde{u}} \right| + \bar{\delta}_{2\gamma}^{\mathrm{MT}} \left(\varepsilon, Q^2 \right) \,, \tag{16}$$

with

$$\bar{\delta}_{2\gamma}^{\mathrm{MT}} = \frac{2\alpha}{\pi} \left\{ \frac{1}{2} \ln^2 \left| \frac{\tilde{s}}{\tilde{u}} \right| - \frac{1}{2} \ln^2 \frac{\tilde{s}}{s} - \mathrm{Li}\left(\frac{\tilde{s}}{s} \right) - \mathrm{Li}\left(\frac{u}{\tilde{u}} \right) + \frac{\pi^2}{3} \right\} \,, \tag{17}$$

where λ^2 is the soft photon mass (IR regulator), $\tilde{s} = s - m^2$, $\tilde{u} = u - m^2$, and $\mathrm{Li}(z)$ is the Spence function (dilogarithm) defined by

$$\mathrm{Li}(z) = -\int_0^z \mathrm{d}t \frac{\ln(1 - t)}{t} \,. \tag{18}$$

Using Eqs. (7) and (16), the r.h.s. in Eq. (15) can be written as

$$\sigma_{\mathrm{R}}^{1\gamma,\mathrm{MT}} = G_{\mathrm{M}}^2 + \frac{\varepsilon}{\tau} G_{\mathrm{E}}^2 + 2 G_{\mathrm{M}} \, \mathrm{Re} \left[\delta \tilde{G}_{\mathrm{M}}^{2\gamma} + \varepsilon \frac{\nu}{m^2} \tilde{F}_3 - G_{\mathrm{M}} \frac{1}{2} \delta_{2\gamma}^{\mathrm{MT}} \right] \,. \tag{19}$$

Let us look at the expression in square brackets in more detail. Substituting the explicit expressions for the amplitudes, we obtain

$$\delta \tilde{G}_{\mathrm{M}}^{2\gamma} + \varepsilon \frac{\nu}{m^2} \tilde{F}_3 - G_{\mathrm{M}} \frac{1}{2} \delta_{2\gamma}^{\mathrm{MT}} =$$

$$-\frac{\alpha}{\pi} \left(\mathcal{F}_1 \left(Q^2 \right) \ln \frac{s}{\mu_{\mathrm{F}}^2} \ln \left| \frac{s}{u} \right| - G_{\mathrm{M}} \left(Q^2 \right) \ln \frac{\tilde{s}}{\mu_{\mathrm{F}}^2} \ln \left| \frac{\tilde{s}}{\tilde{u}} \right| \right) \tag{20}$$

$$+\frac{\alpha}{\pi} \left[\bar{C}_{\mathrm{M}} \left(\varepsilon, Q^2 \right) + \varepsilon \frac{\nu}{s} C_3 \left(\varepsilon, Q^2 \right) \right] \mathcal{F}_1 \left(Q^2 \right) - G_{\mathrm{M}} \frac{1}{2} \bar{\delta}_{2\gamma}^{\mathrm{MT}} \tag{21}$$

$$+\delta \tilde{G}_{\mathrm{M}}^{(h)} \left(\varepsilon, Q^2 \right) + \varepsilon \frac{\nu}{m^2} \tilde{F}_3^{(h)} \left(\varepsilon, Q^2 \right) . \tag{22}$$

From the first line (20), it follows that the IR-regulator λ^2 cancels in the combination of the logarithms as it should be

$$g_1 - G_{\mathrm{M}} \frac{1}{2} \delta_{2\gamma}^{\mathrm{MT}} = \frac{\alpha}{\pi} G_{\mathrm{M}} \ln \frac{\tilde{s}}{\mu_{\mathrm{F}}^2} \ln \left| \frac{\tilde{s}}{\tilde{u}} \right| - G_{\mathrm{M}} \frac{1}{2} \bar{\delta}_{2\gamma}^{\mathrm{MT}} . \tag{23}$$

This gives logarithm $\sim G_{\mathrm{M}} \ln(\tilde{s}/\mu_{\mathrm{F}}^2) \ln |\tilde{s}/\tilde{u}|$ with $s/\mu_{\mathrm{F}}^2 \gg 1$. This large logarithm is proportional to magnetic FF G_{M}, which reflects that this contribution arises from the hard–soft photon configuration. The scale $\mu_{\mathrm{F}} \sim \Lambda$ plays the role of UV cutoff for the soft-photon virtuality. One more large logarithm also appears from the hard–hard photon contribution, see Eq. (A.1). However, its coefficient is proportional to WACS FF $\mathcal{F}_1$. Notice that the coefficients of large logarithms in Eq. (20) vanishe in the forward limit (8), which is provided by the factor $\ln(-u/s) \simeq \ln(1+t/s) \sim t/s$ at large energy $s \to \infty$.

The hard–hard photon domain in the soft-spectator contribution also gives the term $(\bar{C}_{\mathrm{M}} + \varepsilon \frac{\nu}{s} C_3)$ in Eq. (21). This combination of the hard functions also vanishes in the forward limit (8). Fulfilment of this condition provides an important check of the obtained analytical expressions. On the other hand, this leads to a strong numerical cancellation between the large numerical terms in $\bar{C}_{\mathrm{M}}$ and in $\varepsilon \frac{\nu}{s} C_3$.

The hard-spectator contributions $\delta \tilde{G}_{\mathrm{M}}^{(h)}$ and $\frac{\nu}{m^2} \tilde{F}_3^{(h)}$ in (22) independently vanish in the forward limit which follows from the structure of the perturbative kernels. Therefore, the boundary condition (8) is well satisfied. From this observation, it follows that the simple extrapolation of Eq. (19) in the forward limit gives

$$\sigma_{\mathrm{R}}^{1\gamma,\mathrm{MT}} \left(\varepsilon = 1, Q^2 \right) = G_{\mathrm{M}}^2 + \frac{1}{\tau} G_{\mathrm{E}}^2 = G_{\mathrm{M}}^2 \left(1 + \frac{\varepsilon}{\tau} R^2 \right) , \tag{24}$$

where we introduced the ratio $R = G_{\mathrm{E}}/G_{\mathrm{M}}$. Let us rewrite Eq. (19) as

$$\sigma_{\mathrm{R}}^{1\gamma,\mathrm{MT}} = G_{\mathrm{M}}^2 \left(1 + \frac{\varepsilon}{\tau}R^2\right) + 2G_{\mathrm{M}}\,\mathrm{Re}\left[\delta\tilde{G}_{\mathrm{M}}^{2\gamma} + \varepsilon\frac{\nu}{m^2}\tilde{F}_3 - G_{\mathrm{M}}\frac{1}{2}\delta_{2\gamma}^{\mathrm{MT}}\right]\,, \quad (25)$$

where we assume that the ratio R is fixed from the experimental data [29–32]. Then the discrepancy between polarised and unpolarised data can be explained by the TPE contribution in Eq. (25). Let us remind that obtained expressions for the TPE amplitudes are only valid in the region where *all* Mandelstam variables are sufficiently large (1). This means that we cannot describe the backward region where variable u is small. The minimum value of $u_{\min}$ corresponding to the boundary $u > u_{\min}$ is equivalent to the condition $\varepsilon > \varepsilon_{\min}$ and will be considered further.

Many existing data allows one to conclude that behavior of the reduced cross section $\sigma_{\mathrm{R}}^{1\gamma,\mathrm{MT}}(\varepsilon,Q^2)$ at relatively low values of Q^2 can be sufficiently well described by the linear empirical fit

$$\sigma_{\mathrm{R}}^{1\gamma,\mathrm{MT}}\left(\varepsilon,Q^2\right) = a + \varepsilon b\,. \quad (26)$$

For higher values of Q^2, it is assumed that this behaviour also holds for the entire interval $0 < \varepsilon < 1$ at fixed Q^2 that suggests that the non-linear effects in TPE are very small. If this is so, then the empirical constants a and b can be obtained from the data corresponding to the given cross section at fixed Q^2. Combining (24) and (26), one finds [33]

$$G_{\mathrm{M}}^2 = \frac{a + b}{1 + R^2/\tau}\,. \quad (27)$$

The value of G_{M}^2 thus obtained, used in Eq. (25), ensures that the linear behaviour (26) does not contradict to the boundary condition (24).

3. Estimates of TPE effect in elastic electron–proton scattering

In order to perform numerical estimates, let us fix the non-perturbative input in the TPE amplitudes. For the FF $\mathcal{F}_1$, we use the simple empirical parametrisation which was obtained in Ref. [26]

$$\mathcal{F}_1\left(Q^2\right) = \left(\frac{\Lambda^2}{Q^2}\right)^\alpha\,, \quad (28)$$

where $\Lambda = 1.174\,\mathrm{GeV}^2$ and the exponent $\alpha = 2.091$. This FF provides a good description of the measured WACS cross section for different energies s in the interval $2.5\,\mathrm{GeV}^2 < Q^2 < 6.5\,\mathrm{GeV}^2$ and $-u \geq 2.5\,\mathrm{GeV}^2$. This restriction can be easily converted to the boundary for the photon polarisation $\varepsilon_{\min} < \varepsilon < 1$ for a fixed value of Q^2. For the value of the factorisation scale in Eq. (20), we take $\mu_{\mathrm{F}} = 200\,\mathrm{MeV}$.

In order to describe the hard-spectator terms, we take the model for the nucleon distribution amplitude (DA) from Ref. [34]

$$\varphi_3(x_1, x_2, x_3) = 120\, f_N\, x_1 x_2 x_3\, \bar{\varphi}_3(x_i, \mu)\,, \tag{29}$$

$$\bar{\varphi}_3(x_i) = 1 + \sum_{j=0}^{1} \phi_{1j}(\mu) P_{1j}(x_1, x_2, x_3) + \sum_{j=0}^{2} \phi_{2j}(\mu) P_{2j}(x_1, x_2, x_3)\,, \tag{30}$$

where $P_{ij}(x_i)$ are homogenous orthogonal polynomials

$$P_{10}(x_i) = 21(x_1 - x_3)\,, \quad P_{11}(x_i) = 7(x_1 - 2x_2 + x_3)\,, \tag{31}$$

$$P_{20}(x_i) = \frac{63}{10}\left[3(x_1 - x_3)^2 - 3x_2(x_1 + x_3) + 2x_2^2\right]\,, \tag{32}$$

$$P_{21}(x_i) = \frac{63}{2}(x_1 - 3x_2 + x_3)(x_1 - x_3)\,, \tag{33}$$

$$P_{22}(x_i) = \frac{9}{5}\left[x_1^2 + 9x_2(x_1 + x_3) - 12x_1 x_3 - 6x_2^2 + x_3^2\right]\,. \tag{34}$$

The moments $\phi_{ij}(\mu)$ are multiplicatively renormalisable, see more details in Refs. [34, 35]. Their values are estimated with the help of light-cone sum rules for the electromagnetic FFs. For our analysis, we will use the ABO1 model [34] and the COZ model from Ref. [36]. The numerical values for the coefficients ϕ_{ij} are given in Table 1. For the normalisation constant f_N in (29), we use

$$f_N = (5.0 \pm 0.5) \times 10^{-3}\ \text{GeV}^2\,, \tag{35}$$

obtained from the QCD sum rules [36].

Table 1. The numerical values of DA parameters ϕ_{ij} at $\mu^2 = 4\ \text{GeV}^2$.

Model	φ_{10}	φ_{11}	φ_{20}	φ_{21}	φ_{22}
ABO	0.050	0.050	0.075	-0.027	0.170
COZ	0.154	0.182	0.380	0.054	-0.146

The scale of the running coupling $\alpha_s(\mu_R^2)$ is set to be $\mu_R^2 \simeq 0.6\, Q^2$ and we use the two-loop running coupling with $\alpha_s(1.5) = 0.360$.

In our numerical calculations we also use the ratio $R = G_E/G_M$ which is fixed from the experimental data [29–32]. For simplicity, we perform the following empirical fit of the data for the interval 0.5–8.5 GeV^2 in Q^2:

$$R\left(Q^2\right) = \mu_p^{-1}\left(1 - a \ln^2\left[Q^2/\Lambda_R^2\right]\right)\,, \tag{36}$$

with $a = 0.070 \pm 0.007$, $\Lambda_R = 0.54 \pm 0.03$ GeV. The other parameters read $m = 938$ MeV, $\mu_p = 2.7928$.

Combining this input with the linear fit (26), using G_M as in Eq. (25), the analysis of the JLab data from Ref. [37] gives results, which are shown in Fig. 2 and Fig. 3.
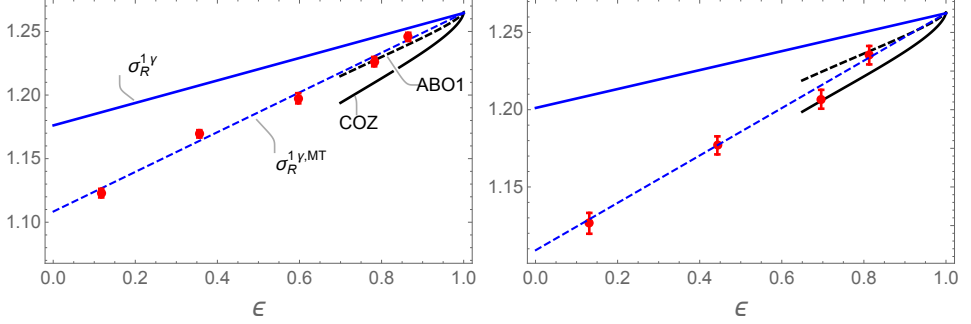

Fig. 2.   The reduced cross section as a function of ε at fixed values of $Q^2 = 2.64, 3.20$ GeV^2, the data are from Ref. [37].
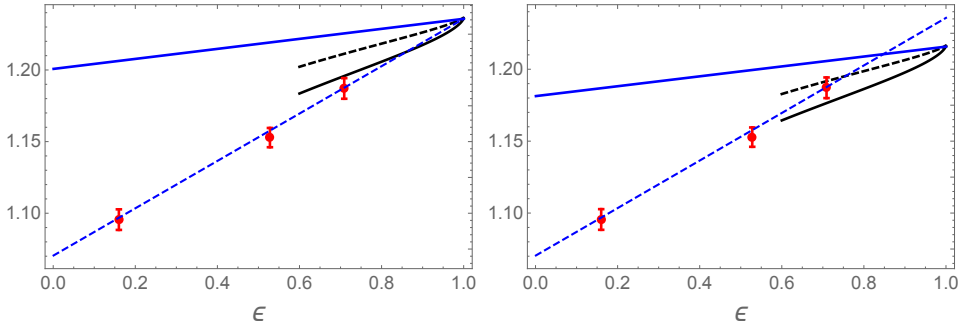

Fig. 3. Left: the reduced cross section as a function of ε at fixed values of $Q^2 = 4.10$ GeV^2, the data are from Ref. [37, 38]. Right: the same but assuming nonlinear behaviour and smaller FF G_M, see more details in the text.

The blue solid line in these figures shows the reduced cross section with the slope obtained from the polarisation transfer experiments. For convenience, the cross section is normalised to the square of the dipole FF $G_\mathrm{dip}(Q^2) = \mu_p/(1 + Q^2/\Lambda^2)^2$, with $\Lambda = 0.71$ GeV^2. The blue dashed line corresponds to the linear fit of the unpolarised data for $\sigma_\mathrm{R}^{1\gamma,\mathrm{MT}}$ (red points).

These lines are extrapolated to the point of $\varepsilon = 0$, where the TPE effect must vanish. The different slopes of these lines must be explained.

The black solid and dashed lines represent the reduced cross section with the TPE contribution for COZ and ABO1 models, respectively. These lines are only shown in the region of $\varepsilon > \varepsilon_\mathrm{min}$, where our approximation is valid.

The numerical value of the TPE effect is sensitive to the choice of the model for nucleon DA. The obtained plots show that TPE with the ABO1 model of DA works reasonably well for $Q^2 = 2.6$ and 3.2 GeV^2 but for $Q^2 = 4.10$ GeV^2, the corresponding numerical effect is already somewhat small. For the COZ model, it gives a large numerical effect: large effect at $Q^2 = 2.6$ GeV^2 and quite reliable description for $Q^2 = 3.2$ and 4.10 GeV^2. Such a result illustrates that the obtained description is sensitive to the hard-spectator contribution, which turns out to be quite large compared to the soft-spectator one.

In order to better understand this point, we plot in Fig. 4 the different contributions for the TPE correction in Eq. (25) for $Q^2 = 4.10$ GeV^2. The TPE contributions are represented as a sum of four terms according to Eqs. (20)–(22). For convenience, we normalise the TPE corrections to the value of R^2/τ. The largest contributions are generated by the logarithms in Eq. (20) (blue dashed line with the label "large Logs") and by the soft-spectator contribution $\left(\bar{C}_\mathrm{M} + \varepsilon \frac{\nu}{s} C_3 \right) \mathcal{F}_1$ (black, dot-dashed line with the label "soft"), which has the opposite sign. The hard-spectator term $\delta \tilde{G}_\mathrm{M}^{(h)} + \varepsilon \frac{\nu}{m^2} \tilde{F}_3^{(h)}$ for the different models is shown by solid (red) curves with the labels "COZ" and "ABO1", respectively. The MT subtraction term $G_\mathrm{M} \bar{\delta}_{2\gamma}^\mathrm{MT}/2$ is shown by black dotted curve.
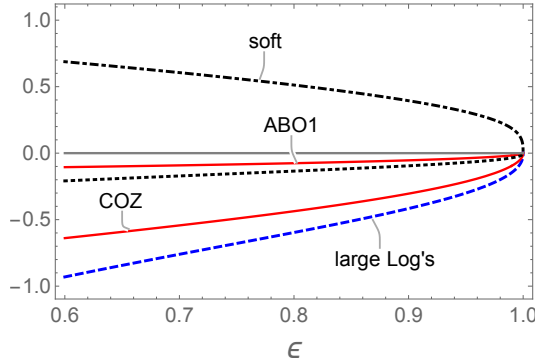

Fig. 4. The various TPE contributions as shown in Eqs. (20)–(22) at fixed $Q^2 = 4.10$ GeV^2. See further explanation in the text.

The soft-spectator contribution is positive, while the combination with large logarithms gives the negative contribution. Together these terms give about -30% effect (relative to R^2/τ) at $\varepsilon_\mathrm{min} = 0.6$. The MT subtraction term gives an additional -10%. However, the resulting correction is still small and in the case of the ABO1 model, such a description gives only half of the required effect. The hard-spectator contribution with the COZ model gives a much larger numerical effect, which is about the factor six

larger compared to the ABO1 model and gives about -60%. This allows one to describe the gap between the polarised and unpolarised linear curves in Fig. 3.

The strong cancellation between the soft-spectator (21) and large logarithm (20) contributions, which makes the overall result to be more sensitive to the hard-spectator term (22), is not accidental. The large positive contribution occurs in the combination of the hard functions $\bar{C}_{\mathrm{M}} + \varepsilon \frac{\nu}{s} C_3$ and is dominated by the simple numerical constant

$$\bar{C}_{\mathrm{M}} + \varepsilon \frac{\nu}{s} C_3 = (1 - \varepsilon) \frac{\pi}{2} + \mathcal{O}\left(s^{-1}\right) . \tag{37}$$

This behaviour ensures the fulfilment of the boundary condition (8). This is an important property of the box diagram in the hard region.

Our numerical estimates show that the obtained TPE effect decreases with increasing Q^2. However, the existing data [18, 48, 49] indicate that the TPE effect remains quite large at large values of Q^2. In order to illustrate this, we show in Fig. 5 the same plots as in Fig. 3 but for $Q^2 = 7$ GeV^2. Notice that in this case, we need to extrapolate the empirical formula (28) for the FF $\mathcal{F}_1$, which also provides additional ambiguity. Nevertheless, from Fig. 5, it is clearly seen that even with the COZ model it is not possible to describe the difference between the different slopes.
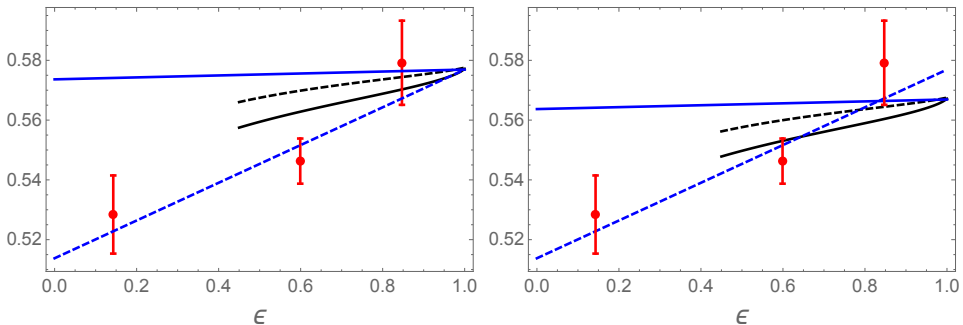

Fig. 5. Left: the same as in Fig. 3, $Q^2 = 7$ GeV^2, the data are from Refs. [18, 48]. Right: the same but assuming nonlinear behaviour and smaller FF G_{M}.

This behaviour may indicate that there is an effect beyond the description developed that needs to be taken into account. This effect is especially important for sufficiently large values of $Q^2 > 4$ GeV^2.

One possible solution is that assumption about the linear ε-behaviour of the reduced cross section on the whole interval must be revised. There are no strict theoretical arguments in favor of the fact that the TPE amplitudes should have a linear behavior in ε over the entire interval. For example, the slope in the region of $\varepsilon > \varepsilon_{\min}$ for large Q^2 may differ from the slope

in the region of $\varepsilon < \varepsilon_{\min}$. The reason for this behaviour may be that the TPE amplitudes depend on completely different underlying scattering mechanisms for small and large values of ε (backward and forward domains, respectively). Then such an effect can play an important role at large values of Q^2. The absolute value of such an effect may be relatively small and therefore may not have a strong impact on the value of G_{M}, but may play an important role in understanding the FF ratio discrepancy.

In such a case, the value of the FF G_{M} cannot be obtained by the simple extrapolation of the linear behaviour to the point of $\varepsilon = 0$ or $\varepsilon = 1$. In order to illustrate the corresponding effect, let us consider a small modification of the calculations in Fig. 3 and Fig. 5, and assume that the slope in the region of $\varepsilon > \varepsilon_{\min}$ approximately agree with our calculations but the value of G_{M} is smaller than the one obtained from the linear fit in the total region of $0 < \varepsilon < 1$. The results are shown in the right plots of the same figures. As a result the value of the FF G_{M} was reduced by 1.7% and 1.3% for $Q^2 = 4.10$ and 7.0 GeV^2, respectively. It is evident that such behaviour allows us to qualitatively understand the discrepancy in the region of $\varepsilon > \varepsilon_{\min}$. This assumption can be verified experimentally by precise measurements of the reduced cross section in the region of $\varepsilon > \varepsilon_{\min}$.

The TPE calculation under discussion involves various uncertainties. These uncertainties can be divided into theoretical and experimental. The latter are associated with the data which are used to estimate non-perturbative quantities, like nucleon DA, $\mathcal{F}_1$. Theoretical ambiguities are related to the various QCD next-to-leading and power corrections, which can provide some effect at moderate values of Q^2.

Thus, one can see that the TPE effect is quite sensitive to the model of the proton DA. The COZ model gives a much larger numerical effect because this distribution is sensitive to the configuration where the spectator quark momentum fraction is small. It is possible that this indicates a large contribution from soft overlap associated with the so-called "cat's ear" configuration, where photons interact with different quarks. Such a contribution has not yet been studied in the literature, since it is suppressed by the inverse power of $1/Q^2$.

The existing lattice and non-perturbative results indicate that the value of the normalisation constant f_{N} can be smaller than the one used in this work, see *e.g.* Refs. [39, 40]. Using such a small value of f_{N} will further suppress the contribution of the hard observer (by about a factor of two), reducing the effect of TPE. At the same time, a smaller value of f_{N} also reduces the pQCD (hard spectator contribution) predictions for nucleon FF and WACS, indicating a larger effect of the soft-spectator mechanism in these hard exclusive reactions.

4. TPE correction in elastic electron–neutron scattering

A discussion of the TPE for the neutron target can also be important for a Rosenbluth analysis of data for reduced cross section at higher values of Q^2. The main difference with the proton is that the TPE amplitude is free from the QED IR-divergency. On the other hand, the contribution of the hard photons remains significant.

The theoretical description of the TPE amplitudes can be carried out in the same way but now we expect that the amplitudes associated with the soft photon are very small

$$\delta_{2\gamma}^{\mathrm{MT}} = 0\,, \qquad g_{1n}\left(\varepsilon, Q^2\right) = 0\,. \tag{38}$$

From existing data [41] one can conclude that at least in the region of $Q^2 < 4\,\mathrm{GeV}^2$, the ratio $R_n = G_{\mathrm{E}n}/G_{\mathrm{M}n}$ is sufficiently small and the estimate in Eq. (6) also works in this case. Therefore, Eq. (19) can be used for the phenomenological estimates.

The required amplitudes, which enter in the expression for the reduced cross section in (19) now reads

$$\delta\tilde{G}_{\mathrm{M}n}^{2\gamma} + \varepsilon\frac{\nu}{m^2}\tilde{F}_{3n} = -\frac{\alpha}{\pi}\mathcal{F}_{1n}\left(Q^2\right)\ln\frac{s}{\mu_{\mathrm{F}}^2}\ln\left|\frac{s}{u}\right|$$
$$+\frac{\alpha}{\pi}\left[\bar{C}_{\mathrm{M}}\left(\varepsilon, Q^2\right) + \varepsilon\frac{\nu}{s}C_3\left(\varepsilon, Q^2\right)\right]\mathcal{F}_{1n}\left(Q^2\right) + \delta\tilde{G}_{\mathrm{M}n}^{(h)} + \varepsilon\frac{\nu}{m^2}\tilde{F}_{3n}^{(h)}\,, \tag{39}$$

where subscript n denotes a neutron amplitude and FFs. The first two terms in the r.h.s. of Eq. (39) correspond to the soft-spectator contribution. The large logarithm arises from the $\delta\tilde{G}_{\mathrm{M}n}^{(s)}$. The hard coefficient functions $\bar{C}_{\mathrm{M}}$ and C_3 are the same as for the proton, see Eqs. (A.2) and (A.3).

The hard-spectator contributions can be described very similar to a proton case, with the difference due to the interchange of the quarks charges $e_u \leftrightarrow e_d$ in the hard amplitudes. The nucleon DA is the same.

The soft-spectator contribution depends on the FF $\mathcal{F}_{1n}$ which is different from the proton FF $\mathcal{F}_1$ due to the different quark electromagnetic charges. This FF can be obtained from the WACS on the neutron like $\mathcal{F}_1$, but such measurements have not yet been done. We get an estimate of this quantity using the isotopic symmetry, nucleon electromagnetic FFs, and WACS FF $\mathcal{F}_1$ obtained for the proton. The current data allows one to get the values of $\mathcal{F}_{1n}$ for $Q^2 = 2.5$ and $3.4\,\mathrm{GeV}^2$. The details are provided in Appendix C. These calculations give

$$\mathcal{F}_{1n}(2.5) \simeq 0.25\,, \qquad \mathcal{F}_{1n}(3.4) \simeq 0.12\,. \tag{40}$$

The reduced cross section for a neutron target reads

$$\sigma_{\mathrm{R}n} = G_{\mathrm{M}n}^2\left(1 + \frac{\varepsilon}{\tau}R_n^2\right) + 2G_{\mathrm{M}n}\,\mathrm{Re}\left[\delta\tilde{G}_{\mathrm{M}n}^{2\gamma} + \varepsilon\frac{\nu}{m^2}\tilde{F}_{3n}\right]\,. \tag{41}$$

We take the value of the ratio R_n from the data in Ref. [41]

$$\mu_n R_n(2.5) = 0.397 \,, \qquad \mu_n R_n(3.4) = 0.481, \qquad (42)$$

where the neutron magnetic moment $\mu_n = -1.913$. The values of the FF $G_{\mathrm{M}n}$ are taken from Ref. [42]

$$G_{\mathrm{M}n}(2.5) = 0.0506 \, \mu_n \,, \qquad G_{\mathrm{M}n}(3.4) = 0.0296 \, \mu_n \,. \qquad (43)$$

The obtained TPE effect is shown in Fig. 6. We show the results in the $\varepsilon > \varepsilon_{\min}$ region only. The solid blue line gives the reduced cross section without the TPE contribution. The black dashed and solid lines describe the reduced cross section with the TPE effect for the ABO1 and COZ models of the nucleon DA, respectively. The big difference for the different models is explained by the cancellation between the soft-spectator (which is positive) and the hard-spectator contribution. Taking into account the experience with the proton cross section, we expect that the ABO1 model provides a more realistic description. In this case, the hard-spectator contribution is relatively small and the obtained numerical effect is about 2.2–2.5% relative to the Born cross section. Such a correction is comparable with the one in the proton case but it has the opposite sign. This reduces the slope, providing the smaller ratio R_n. The obtained estimates are applicable for a small region of $\varepsilon > \varepsilon_{\min}$, however, it can be assumed that the TPE effect will be even greater in the region of large ε, as follows from the estimates of the hadron model [7]. Therefore, the TPE correction for the neutron cross section is also important and should be taken into account when analysing the experimental data.
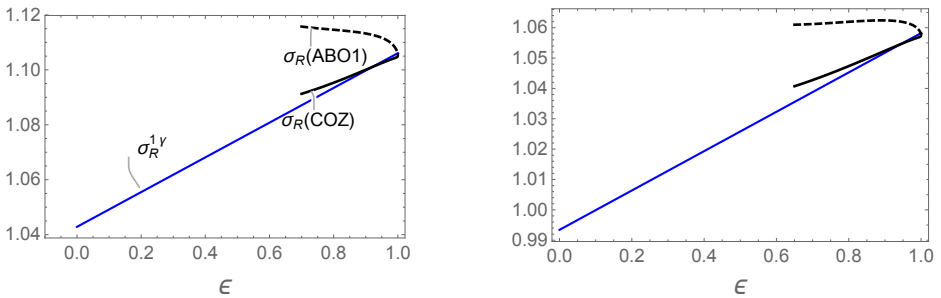

Fig. 6. The normalised reduced cross section $\sigma_{\mathrm{R}}/(\mu_n G_{\mathrm{dip}})^2$ as a function of ε at fixed values of $Q^2 = 2.5$ (left) and 3.4 GeV^2 (right). The solid blue curve corresponds to the one-γ exchange with the ratios R_n from Eq. (42). The black dashed and solid lines describe the cross section with the different TPE contributions.

5. Discussion

Motivated by measurements at large Q^2, we reanalyse the TPE effect in elastic electron–proton scattering. We use the effective field theory formalism developed in Ref. [25]. This description is different from the existing hadronic and dispersive approaches because it systematically separates and includes the short- and long-distance effects. The short-distance amplitudes are computed in pQCD, the long-distance quantities are restricted using different experimental data or a low-energy EFT. The resulting description works only in the region where all kinematic variables are large (1). In other words, for a fixed Q^2, the formalism is applicable only in a certain region of $\varepsilon > \varepsilon_{\min}$. The value of $\varepsilon_{\min}$ depends on the energy and momentum transfer and $\varepsilon_{\min} \to 0$ as $Q^2 \to \infty$.

The developed formalism takes into account the soft- and hard-spectator contributions, which are associated with the different underlying hard scattering of the quarks. It is shown that there are strong cancellations between different large terms in the TPE amplitudes. It is also found that at large Q^2, the contribution of excited hadronic states is strongly suppressed in the region where one photon is soft. As a result, the value of the TPE effect is quite sensitive to the so-called "cat's ear" diagrams, which have been computed in the hard-spectator approximation. We perform a numerical analysis using two different models for the nucleon distribution amplitude.

The developed description allows us to explain the discrepancy between the FF data using TPE for $Q^2 = 2.5$–3.5 GeV^2, but for larger Q^2, the obtained TPE correction is no longer large enough, provided that the cross section depends linearly on the photon polarisation. Probably, the basic assumption about the linear behaviour of the reduced cross section with respect to ε over the entire interval for fixed Q^2 should be critically revised for large values of Q^2. The different behavior can be naturally explained by the different scattering dynamics in the region of small $\varepsilon < \varepsilon_{\min}$ and large $\varepsilon > \varepsilon_{\min}$ photon polarisation.

We show that using a different slope in the $\varepsilon > \varepsilon_{\min}$ region changes the extracted G_{M} value by 1–2% for $Q^2 \leq 7$ GeV^2, but they also have a strong effect on the extracted small $G_{\mathrm{E}}/G_{\mathrm{M}}$ ratio. Note that some non-linearities were also observed in the dispersion calculations of $Q^2 < 5$ GeV^2 [16].

The developed formalism has been used to estimate the TPE effect in the electron–neutron scattering. In this case, the long-distance effects associated with the soft-photon interaction are absent and the dominant contribution is only associated with the hard photons. However, the specific hard-collinear FF $\mathcal{F}_{1n}$, which is defined within the SCET framework and describes the soft-spectator scattering, cannot be restricted from the data as in the case of a proton target. Therefore we use isospin symmetry and existing data for the proton and neutron electromagnetic FFs in order to estimate this

quantity. Our estimates for $Q^2 = 2.5$–3.5 GeV^2 allow us to conclude that the obtained TPE effect is quite large and comparable to that in the proton cross section.

Appendix A

Analytical expressions for the soft- and hard-spectator TPE amplitudes

For convenience, we provide the analytical expressions for the amplitudes used in the paper

$$\delta \tilde{G}_{\mathrm{M}}^{(s)}\left(\varepsilon, Q^2\right) + \varepsilon \frac{\nu}{m^2} \tilde{F}_3^{(s)} = \frac{\alpha}{\pi}\, g_1\left(\varepsilon, Q, \mu_{\mathrm{F}}\right) + \frac{\alpha}{\pi} \ln \left|\frac{u}{s}\right| \mathcal{F}_1\left(Q^2\right) \ln \frac{s}{\mu_{\mathrm{F}}^2}$$

$$+ \frac{\alpha}{\pi} \left\{ \bar{C}_{\mathrm{M}}\left(\varepsilon, Q^2\right) + \frac{\nu}{s} C_3\left(\varepsilon, Q^2\right) \right\} \mathcal{F}_1\left(Q^2\right) . \quad \text{(A.1)}$$

The hard coefficient functions read

$$\bar{C}_{\mathrm{M}}\left(\varepsilon, Q^2\right) = \frac{1}{2} \ln^2 \bar{z} - \frac{1}{4} \frac{z \ln^2 z}{1-z} - \frac{z \ln^2 \bar{z}/z}{4} - \frac{1}{2} \ln \bar{z} + \frac{2-z}{4} \pi^2 , \quad \text{(A.2)}$$

$$C_3\left(z, Q^2\right) = \frac{2-z}{2\bar{z}^2} \ln^2 z - \frac{2-z}{2} \ln^2 \frac{\bar{z}}{z} + \frac{1}{\bar{z}} \ln z + \ln \frac{\bar{z}}{z} - \frac{2-z}{2} \pi^2 , \quad \text{(A.3)}$$

where $z = -t/s > 0$. These expressions are in agreement with the analogous calculations in Ref. [24].

The hard-spectator contribution for the proton case reads[2]

$$\delta \tilde{G}_{\mathrm{M}}^{(h)} = -\frac{\alpha\, \alpha_{\mathrm{s}}\left(\mu^2\right)}{Q^4} \left(\frac{4\pi}{3!}\right)^2 \frac{1}{2}(2\zeta - 1)\, J_{\mathrm{M}}(\zeta) , \quad \text{(A.4)}$$

$$\frac{\nu}{M^2} \tilde{F}_3^{(h)} = -\frac{\alpha\, \alpha_{\mathrm{s}}\left(\mu^2\right)}{Q^4} \left(\frac{4\pi}{3!}\right)^2 \frac{1}{2}(2\zeta - 1)\, J_3(\zeta) , \quad \text{(A.5)}$$

where $\zeta = 1/z = s/(-t) > 1$. The convolution integrals read

$$J_{\mathrm{M}} = \int \frac{Dy_i}{y_1 y_2 \bar{y}_2} \int \frac{Dx_i}{x_1 x_2 \bar{x}_2} \frac{4\, x_2\, y_2}{D_2[\zeta] D_2[\bar{\zeta}]} \left\{ e_u^2 \left[(V'+A')(V+A) + 4T'T\right](3,2,1)\right.$$
$$\left. + e_u e_d \left[(V'+A')(V+A) + 4T'T\right](1,2,3) + e_u e_d\, 2 \left[V'V + A'A\right](1,3,2) \right\} , \quad \text{(A.6)}$$

$$J_3 = \int \frac{Dy_i}{y_1 y_2 \bar{y}_2} \int \frac{Dx_i}{x_1 x_2 \bar{x}_2} \frac{2(x_2\, \bar{y}_2 + \bar{x}_2\, y_2)}{D_2[\zeta] D_2[\bar{\zeta}]} \left\{ e_u^2 \left[(V'+A')(V+A) + 4T'T\right](3,2,1)\right.$$
$$\left. + e_u e_d \left[(V'+A')(V+A) + 4T'T\right](1,2,3) + e_u e_d\, 2 \left[V'V + A'A\right](1,3,2) \right\} , \quad \text{(A.7)}$$

---

[2] These expressions have an additional factor $1/2$ compared to ones in Ref. [20], where this factor was overlooked.

where

$$Dy_i = dy_1\, dy_2\, dy_3\, \delta(1 - y_1 - y_2 - y_3)\,, \qquad (\text{A.8})$$

quark charges $e_u = +2/3$, $e_d = -1/3$, $\alpha = e^2/(4\pi)$, and $\alpha_s(\mu^2)$ is the strong coupling constant evaluated at scale μ^2. The factor D_2 in the denominator reads

$$D_2[\zeta] = x_2\bar{\zeta} + y_2\zeta - x_2 y_2 + i\varepsilon\,, \qquad \zeta = \frac{1}{z} = \frac{s}{-t} > 1\,. \qquad (\text{A.9})$$

The nucleon DAs

$$V(x_1, x_2, x_3) \equiv V(1,2,3) = \frac{1}{2}\left(\varphi_3 2,1,3) + \varphi_3(1,2,3)\right)\,, \qquad (\text{A.10})$$

$$A(1,2,3) = \frac{1}{2}\left(\varphi_3(2,1,3) - \varphi_3(1,2,3)\right)\,, \qquad (\text{A.11})$$

$$T(1,2,3) = \frac{1}{2}\left[V - A\right](1,3,2) + \frac{1}{2}\left[V - A\right](2,3,1)\,, \qquad (\text{A.12})$$

where the twist-3 DA φ_3 is given in Eq. (29). The products of the DAs in Eqs. (A.6) and (A.7) must be understood as

$$\left[V'V + A'A\right](1,3,2) = V'(1,3,2)V(1,3,2) + A'(1,3,2)A(1,3,2)\,, \qquad (\text{A.13})$$

with

$$V'(1,3,2) \equiv V(y_1, y_3, y_2)\,, \qquad V(1,3,2) \equiv V(x_1, x_3, x_2)\,. \qquad (\text{A.14})$$

The expressions for the neutron amplitudes can be obtained from Eqs. (A.6) and (A.7) interchanging the quark charges $e_u \leftrightarrow e_d$.

Appendix B

The amplitude g_1 within the EFT framework

The function g_1 describes the contribution associated with the region where one of the photons is soft and the other is hard. We assume that in this case, the virtual quark in the box diagram in Fig. 1 has still a sufficiently small virtuality and the interaction with the soft photon is described as a non-perturbative matrix element

$$\langle p', k' | O_+^{\mu}\; \bar{\psi}(0)\gamma_{\mu}\psi(0) | k, p\rangle_{\text{EFT}} = \bar{u}\left(k'\right)\gamma_{\mu}u(k)\; \bar{N}'$$
$$\times \left[\gamma^{\mu}f_1\left(Q^2\right) + \gamma_{\sigma}\frac{\alpha}{\pi}\left(g_{\perp}^{\sigma\mu}g_1(\varepsilon, Q, \mu_{\text{F}}) + \frac{k_{\perp}^{\sigma}k_{\perp}^{\mu}}{|k_{\perp}^2|}\;\frac{\alpha}{\pi}g_3(\varepsilon, Q)\right) + \dots\right]N\,, \tag{B.1}$$

where dots denote the possible chiral-odd structures that are not relevant now. Here, the operator O_+^{μ} is constructed in SCET from the hard-collinear

fields, see the explicit expression in Eq. (C.5). The operator $\bar{\psi}(0)\gamma_\mu\psi(0)$ describes the lepton current. In the leading-order of electromagnetic coupling $\alpha = 0$, Eq. (B.1) gives a matrix element that describes the soft-spectator contribution within the SCET framework. The soft photon exchange leads to the two additional amplitudes $g_{1,3}$ in the r.h.s. of Eq. (B.1). The subscript EFT indicates that the matrix element is understood in the effective field theory, which describes the interaction of the collinear hadrons with soft photon.

In order to compute such a matrix element, one needs an effective field framework. The hard subprocess in this picture is described by the interaction of the hard photon with the partons inside the nucleon. Integration over hard modes gives the operator O_+^μ describing the $\gamma^*p \to p$ or $\gamma^*p \to R$ vertices, where R denotes an excited nucleon state. We will assume that the partons after hard interactions hadronise to a hadron, which interacts with the soft photon like a point-like particle. Corresponding vertex $\gamma R \to p$ must be considered as a part of the soft subprocess. The soft photon cannot resolve the structure of hadrons and interacts with the total charge of a point-like particle. Therefore, the corresponding vertex can be approximated by the FF at zero momentum transfer. The virtuality of the soft photon in this framework is restricted by the value of factorisation scale μ_F, which separates the hard–hard and hard–soft photon–photon configurations.

This effective field theory is very close in spirit to the well-known hadronic model up to one point: computing the diagrams with the hadronic intermediate state, we assume that the virtualities of the particles in such an effective theory cannot be large. In order to guarantee this requirement, we neglect the small photon momentum components in the denominators of the propagators. This can be understood as an expansion of the integrands in the diagrams of the hadronic model. This is somewhat similar to the calculation of Mo and Tsai, except that we also expand the denominators. The obtained integrals have UV divergencies, which must be absorbed into the evolution of the hard coefficient functions (which can be considered as constants in the low-energy EFT).

In Ref. [25], only the elastic contribution was calculated, which yields equation (13). This term includes the QED IR-logarithm, which must cancel in the cross section. The function g_{1R} in Eq. (13) includes the inelastic contributions.

Here, we recalculate the function g_1 and discuss the role of the resonance contributions. We start our consideration from the elastic term and reproduce the result in Eq. (13). We will perform our calculation using the expansion of the hadronic diagrams. There are two diagrams which give four contributions as shown in Fig. 7. The hard photon is shown with red colour, the red blob denotes the hard vertex. Consider the elastic contribution

$$\langle p', k' | O_+^\mu \; \bar{\psi}\gamma_\mu\psi | k, p\rangle_{\text{EFT,el}} = G_{\text{F}} \int\limits_S \mathrm{d}l \; \bar{u}\left(k'\right)$$

$$\times \left[\gamma_\nu \frac{(k'+l)}{(k'+l)^2}\gamma_\mu + \gamma_\mu \frac{(k-l)}{(k-l)^2}\gamma_\nu\right] u(k) \frac{1}{l^2 - \lambda^2} \frac{1}{(q-l)^2}\left(M_{p1}^{\mu\nu} + M_{p2}^{\mu\nu}\right), \quad (\text{B.2})$$

where, for simplicity, the factor G_{F} absorbs various factors from the Feynman rules and the photon mass λ^2 is used for the IR-regularisation. The functions $M_{pi}^{\mu\nu}$ describe the hadronic subdiagrams of the first and second lines in Fig. 7, respectively. The symbol $\int_S \mathrm{d}^4 l$ in (B.2) implies that we perform integration over the region of the soft photon momentum $l \lesssim \mu_{\text{F}} \sim \Lambda$. This means that one must expand the integrand with respect to small l in order to avoid the contributions with $l \gg \Lambda$. Such a framework can be understood as a construction of the effective field theory using the method known as the expansion by regions [43, 44]. The expansion of the integrand produces UV-divergent integrals, which are defined with the help of dimensional regularisation.
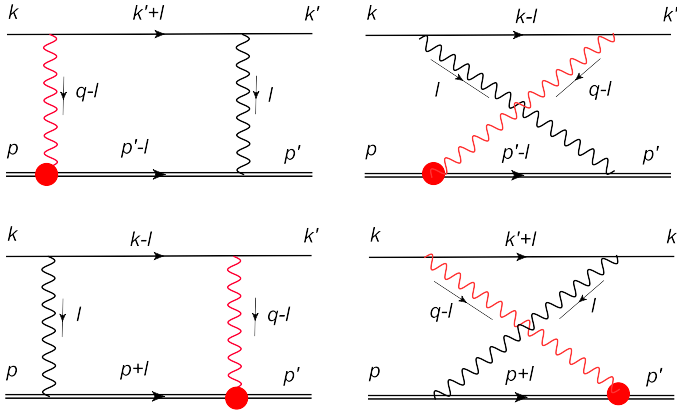

Fig. 7. The diagrams with the hard-soft photons. The hard lines are shown with red colour.

Let us remind that we use in our description the Breit frame, in which the initial and final proton moves along the z-axis and

$$p' = p'_- \frac{n}{2} + \frac{m}{p'_-} \frac{\bar{n}}{2}, \qquad p'_- \sim Q, \quad (\text{B.3})$$

$$p = \frac{m}{p_+} \frac{n}{2} + p_+ \frac{\bar{n}}{2}, \qquad p_+ \sim Q. \quad (\text{B.4})$$

Here, $n = (1,0,0,-1)$ and $\bar{n} = (1,0,0,1)$ are the auxiliary light-cone vectors and $V_\pm = V_0 \pm V_3$ as usually.

The EFT framework implies that the nucleon spinors $\bar{N}(p')$ and $N(p)$ are reduced to the large components $\bar{N}'$ and N, respectively, which are defined as

$$\bar{N}' = \bar{N}(p')\frac{\not{n}\not{n}'}{4}, \qquad N = \frac{\not{n}\not{n}'}{4}N(p). \qquad (B.5)$$

Performing the expansion with respect to the small photon momentum l, we are neglecting all scalar products with small scales in the hard propagators, for instance,

$$(q-l)^2 \simeq q^2, \qquad (B.6)$$

where we neglected $l^2 \sim \Lambda^2$ and $(ql) \sim \Lambda Q$ compared to large (hard) q^2. We assume that the hard interactions are described within the pQCD. In the hard-collinear lines, we neglect soft terms

$$\frac{1}{(p+l)^2 - m^2} \simeq \frac{1}{2(lp)}. \qquad (B.7)$$

In the following, we suppose that the long-distance physics is associated with hard-collinear $\Lambda Q \sim m$ and soft Λ^2 scales. This is valid only for moderate values of Q^2, which guarantee that the hard-collinear scale is sufficiently small. As a result, corresponding dynamics can be associated with hadronic degrees of freedom. The virtualities of the corresponding particles in the hadronic loop cannot be higher than the hard-collinear scale. This restriction is provided by the expansion of the integrand

$$F\left(l, p, p'\right) \simeq F^{(\mathrm{lo})}\left[l^2, (lp), (lp')\right] + \mathcal{O}(l/Q), \qquad (B.8)$$

where $F^{(\mathrm{lo})}$ depends on the appropriate scalar products only. After that, we can skip the restriction S in the loop integral and integrate over all phase space using the dimensional regularisation for treatment of the UV divergencies

$$\int\limits_{S} \mathrm{d}^4 l \, F\left(l, p, p'\right) \simeq \int \mathrm{d}^D l \, F^{(\mathrm{lo})}\left[l^2, (lp), (lp')\right], \qquad D = 4 - 2\varepsilon. \quad (B.9)$$

These UV divergencies must be understood in a sense of low-energy effective field theory.

Performing expansion of the integrand in Eq. (B.2) with respect to small photon momentum l, we find

$$\langle p', k' | \, O_+^\mu \bar{\psi}\gamma_\mu\psi \, | k, p \rangle_{\mathrm{EFT,el}} \simeq G_{\mathrm{F}} \frac{\bar{u}'\gamma_\mu u}{q^2} \int \mathrm{d}^D l$$

$$\left[\frac{k'_\nu}{(k'l)} + \frac{k_\nu}{-(kl)}\right] \frac{1}{l^2 - \lambda^2} \left(M_{p1}^{\mu\nu} + M_{p2}^{\mu\nu}\right), \qquad (B.10)$$

with

$$M_{p1}^{\mu\nu} = \bar{N}' \left\{ \gamma^\nu G_{\mathrm{M}}(0) - \frac{p'^\nu + l^\nu/2}{m} F_2(0) \right\} \frac{(p' - l + m)}{(p' - l)^2 - m^2} \left\{ G_{\mathrm{M}} \left(Q^2 \right) \gamma_\perp^\mu \right\} N \tag{B.11}$$

$$\simeq G_{\mathrm{M}} \left(Q^2 \right) \bar{N}' \gamma_\perp^\mu N \left\{ G_{\mathrm{M}} \frac{p'^\nu}{-(p'l)} - \frac{p'^\nu + l^\nu/2}{-(p'l)} F_2 \right\} \tag{B.12}$$

$$= G_{\mathrm{M}} \left(Q^2 \right) \bar{N}' \gamma_\perp^\mu N \left[F_1 \frac{p'^\nu}{-(p'l)} - \frac{l^\nu}{-(p'l)} \frac{1}{2} F_2 \right]. \tag{B.13}$$

The similar consideration yields

$$M_{p2}^{\mu\nu} = G_{\mathrm{M}} \left(Q^2 \right) \bar{N}' \gamma_\perp^\mu N \left[F_1 \frac{p^\nu}{(pl)} + \frac{l^\nu}{(pl)} \frac{1}{2} F_2 \right]. \tag{B.14}$$

Taking into account the gauge invariance

$$\left[\frac{k'_\nu}{(k'l)} + \frac{k_\nu}{-(kl)} \right] l^\nu = 0, \tag{B.15}$$

and normalisation $F_1(0) = 1$, we obtain

$$M_{1h}^{\mu\nu} + M_{2h}^{\mu\nu} = G_{\mathrm{M}} \left(Q^2 \right) \bar{N}' \gamma_\perp^\mu N \left[\frac{p^\nu}{(pl)} + \frac{p'^\nu}{-(p'l)} \right]. \tag{B.16}$$

Therefore, we find

$$\langle p', k' | O_+^\mu \ \bar{\psi} \gamma_\mu \psi | k, p \rangle_{\mathrm{EFT,el}} \simeq G_{\mathrm{F}} \frac{\bar{u}' \gamma_\mu u}{q^2} \bar{N}' \gamma_\perp^\mu N \ G_{\mathrm{M}} \left(Q^2 \right)$$

$$\times \int \frac{\mathrm{d}^D l}{l^2 - \lambda^2} \left[\frac{k'_\nu}{(k'l)} + \frac{k_\nu}{-(kl)} \right] \left[\frac{p^\nu}{(pl)} + \frac{p'^\nu}{-(p'l)} \right]. \tag{B.17}$$

Calculation of the integrals in (B.17) gives expression in Eq. (13).

Consider now inelastic contribution with the resonance $J^P = \frac{1}{2}^-$. The transition vertices are described as [45]

$$V_{\gamma p \to R}^\mu = G_1 \left(Q^2 \right) \left(q^\sigma q^\mu - q^2 g^{\mu\sigma} \right) \gamma_\sigma + G_2 \left(Q^2 \right) \left[q^\sigma \bar{P}^\nu - \left(\bar{P} q \right) g^{\mu\sigma} \right] \gamma_\sigma, \tag{B.18}$$

where q is incoming photon momentum and $\bar{P} = \frac{1}{2}(p + p')$. This gives

$$\langle p', k' | O_+^\mu \ \bar{\psi} \gamma_\mu \psi | k, p \rangle_{\mathrm{EFT}} \Big|_{\frac{1}{2}^-} \simeq G_{\mathrm{F}} \frac{\bar{u}' \gamma^\mu u}{q^2} \int \mathrm{d} l$$

$$\times \left[\frac{k'_\nu}{(k'l)} + \frac{k_\nu}{-(kl)} \right] \frac{1}{l^2} \left(M_{\mathrm{R}1}^{\mu\nu} + M_{\mathrm{R}2}^{\mu\nu} \right), \tag{B.19}$$

with

$$M_{\mathrm{R1}}^{\mu\nu} \simeq G_1(0) \left(l^\sigma l^\nu - l^2 g^{\nu\sigma} \right) \, \bar{N}'\gamma_\sigma \frac{(\not{p}' - \not{l} + m_{\mathrm{R}})}{(p'-l)^2 - m_{\mathrm{R}}^2} \left\{ Q^2 G_1\left(Q^2\right) \gamma_\perp^\mu \right\} N$$

$$+ G_2(0) \left\{ l^\sigma \bar{P}^\nu - \left(\bar{P}l \right) g^{\nu\sigma} \right\} \bar{N}'\gamma_\sigma \frac{(\not{p}' - \not{l} + m_{\mathrm{R}})}{(p'-l)^2 - m_{\mathrm{R}}^2} \left\{ -q^2 G_1\left(Q^2\right) \gamma_\perp^\mu \right\} N \,, \quad \text{(B.20)}$$

where

$$\Delta^2 = m_{\mathrm{R}}^2 - m^2 \,, \qquad \bar{P} = p' - l/2 \,. \quad \text{(B.21)}$$

The similar expression also holds for $M_{\mathrm{R2}}^{\mu\nu}$. Consider the expansion with respect to small l. The first line in r.h.s. of (B.20) gives

$$G_1(0) \left(l^\sigma l^\nu - l^2 g^{\nu\sigma} \right) \, \bar{N}'\gamma_\sigma \frac{(\not{p}' - \not{l} + m_{\mathrm{R}})}{(p'-l)^2 - m_{\mathrm{R}}^2} \gamma_\perp^\mu N \quad \text{(B.22)}$$

$$\simeq \, \bar{N}'\gamma_\perp^\mu N \, G_1(0) \frac{(lp') \, l^\nu - l^2 p'^\nu}{-2 \left(p'l \right) - \Delta^2} \,. \quad \text{(B.23)}$$

In the expansion of the hard-collinear propagator, we keep the mass difference Δ^2 because numerically this difference is of the order of the hard-collinear scale. The contribution with l^ν vanishes due to contraction as in Eq. (B.15). The term with l^2 gives the scaleless integral

$$\int \mathrm{d}l \, \left[\frac{k'_\nu}{(k'l)} + \frac{k_\nu}{-(kl)} \right] \frac{p'^\nu}{-2(p'l) - \Delta^2} = 0 \,. \quad \text{(B.24)}$$

These integrals are scaleless with respect to transverse components $\mathrm{d}^{D-2}l_\top$[3], which can be easily obtained performing the light-cone expansion with respect to external momenta in each case. Therefore, integral (B.24) vanishes.

The second line in Eq. (B.20) gives

$$\left\{ l^\sigma \bar{P}^\nu - \left(\bar{P}l \right) g^{\nu\sigma} \right\} \bar{N}'\gamma_\sigma \frac{(\not{p}' - \not{l} + m_{\mathrm{R}})}{(p'-l)^2 - m_{\mathrm{R}}^2} \gamma_\perp^\mu N \quad \text{(B.25)}$$

$$\simeq \frac{\left(l^\sigma \bar{P}^\nu - \left(\bar{P}l \right) g^{\nu\sigma} \right) p'_\sigma}{-2 \left(p'l \right) - \Delta^2} \, \bar{N}'\gamma_\perp^\mu N + \frac{\left(l^\sigma \bar{P}^\nu - \left(\bar{P}l \right) g^{\nu\sigma} \right)}{-2 \left(p'l \right) - \Delta^2} \bar{N}'\gamma_\sigma \, \not{l}\gamma_\perp^\mu N \,. \quad \text{(B.26)}$$

The first term in (B.26) gives

$$\left(l^\sigma \bar{P}^\nu - \left(\bar{P}l \right) g^{\nu\sigma} \right) 2p'_\sigma = \frac{1}{2} \left[l^2 p'^\nu - (lp') \, l^\nu \right] \,, \quad \text{(B.27)}$$

---

[3] We reserve the symbol $\perp$ for the transverse component with respect to n and $\bar{n}$ vectors in (B.3) and (B.4). For other light-cone basis vectors, we use symbol $\top$.

which also yields the scaleless integrals as in Eq. (B.24). The second term in (B.26) gives

$$\frac{\left(l^\sigma \bar{P}^\nu - \left(\bar{P}l\right) g^{\nu\sigma}\right) l^\lambda}{-2\left(p'l\right) - \Delta^2} \bar{N}' \gamma_\sigma \gamma_\lambda \gamma_\perp^\mu N \tag{B.28}$$

$$= \frac{\left(l^2 \bar{P}^\nu - \left(\bar{P}l\right) l^\nu\right)}{-2\left(p'l\right) - \Delta^2} \bar{N}' \gamma_\perp^\mu N + \frac{-\left(\bar{P}l\right) g^{\nu\sigma} l^\lambda}{-2\left(p'l\right) - \Delta^2} \frac{1}{2} \bar{N}' \left[\gamma_\sigma, \gamma_\lambda\right] \gamma_\perp^\mu N \tag{B.29}$$

$$\simeq \frac{-\left(p'l\right) g^{\nu\sigma} l^\lambda}{-2\left(p'l\right) - \Delta^2} \frac{1}{2} \bar{N}' \left[\gamma_\sigma, \gamma_\lambda\right] \gamma_\perp^\mu N \,, \tag{B.30}$$

where we again neglected the terms with l^2 and l^ν. The remaining term gives

$$\frac{\bar{u}' \gamma_\mu u}{q^2} \int \mathrm{d}l \left[\frac{k'_\nu}{(k'l)} + \frac{k_\nu}{-(kl)}\right] \frac{1}{l^2} M_{N1}^{\mu\nu} \tag{B.31}$$

$$\sim \frac{\bar{u}' \gamma^\mu u}{-Q^2} \frac{1}{2} \bar{N}' \gamma_\perp^\mu \left[\gamma_\lambda, \gamma_\nu\right] N \int \mathrm{d}l \left[\frac{k'^\nu}{(k'l)} + \frac{k^\nu}{-(kl)}\right] \frac{1}{l^2} \frac{-\left(lp'\right) l^\lambda}{-2\left(p'l\right) - \Delta^2} \tag{B.32}$$

$$\sim \frac{\bar{u}' \gamma^\mu u}{-Q^2} \frac{1}{2} \bar{N}' \gamma_\perp^\mu \left[\gamma_\lambda, \gamma_\nu\right] N \frac{\Delta^2}{2} \int \mathrm{d}l \left[\frac{k'^\nu}{(k'l)} + \frac{k^\nu}{-(kl)}\right] \frac{1}{l^2} \frac{l^\lambda}{-2\left(p'l\right) - \Delta^2} , \tag{B.33}$$

where we neglected the scaleless integral

$$\int \mathrm{d}l \left[\frac{k'^\nu}{(k'l)} + \frac{k^\nu}{-(kl)}\right] \frac{1}{l^2} = 0 \,. \tag{B.34}$$

In order to analyse the remnant terms, we perform the light-cone expansions of the l^λ assuming in the numerator $p'^2 \simeq 0$, $k^2 \simeq 0$, $k'^2 \simeq 0$

$$l^\lambda = p'^\lambda \frac{(kl)}{(p'k)} + k^\lambda \frac{(lp')}{(p'k)} + l_\top^{\lambda'}, \tag{B.35}$$

$$l^\lambda = p'^\lambda \frac{(k'l)}{(p'k')} + k'^\lambda \frac{(lp')}{(p'k')} + l_\top^{\lambda'} \,. \tag{B.36}$$

The terms with transverse component $l_\top$ vanish due to rotation invariance. The terms with $k^\sigma k^\lambda$ and $k'^\sigma k'^\lambda$ vanish because of contraction with $\bar{N}' \gamma_\perp^\mu \left[\gamma^\lambda, \gamma^\nu\right] N$. Hence, we only get the combinations

$$p'^\lambda \left[\frac{k'^\nu}{(p'k')} - \frac{k^\nu}{(p'k)}\right] \int \mathrm{d}^D l \, \frac{1}{l^2} \frac{1}{-2\left(p'l\right) - \Delta^2} \,. \tag{B.37}$$

The contraction of the Lorentz indices yields

$$\bar{N}' \gamma_\perp^\mu \left[\gamma_\lambda, \gamma_\nu\right] N \, p'^\lambda \left[\frac{k'^\nu}{(p'k')} - \frac{k^\nu}{(p'k)}\right] = -\bar{N}' \gamma_\perp^\mu \gamma_\nu \not{p}' N \left[\frac{k'^\nu}{(p'k')} - \frac{k^\nu}{(p'k)}\right] \tag{B.38}$$

$$= -\bar{N}' \gamma_\perp^\mu N \, 2p'_\nu \left[\frac{k'^\nu}{(p'k')} - \frac{k^\nu}{(p'k)}\right] = 0 \,. \tag{B.39}$$

Therefore,

$$G_{\rm F} \, \frac{\bar{u}' \gamma_\mu u}{q^2} \int {\rm d}^D l \left[\frac{k'_\nu}{(k'l)} + \frac{k_\nu}{-(kl)} \right] \frac{1}{l^2} M_{\rm R1}^{\mu\nu} = 0 \,. \tag{B.40}$$

The similar analysis for the second contribution with $M_{\rm R2}^{\mu\nu}$ in Eq. (B.19) gives

$$G_{\rm F} \, \frac{\bar{u}' \gamma_\mu u}{q^2} \int {\rm d}^D l \left[\frac{k'_\nu}{(k'l)} + \frac{k_\nu}{-(kl)} \right] \frac{1}{l^2} M_{\rm R2}^{\mu\nu} = 0 \,. \tag{B.41}$$

Therefore,

$$\langle p', k' | \, O_+^\mu \, \bar{\psi} \gamma^\mu \psi \, | k, p \rangle_{\rm EFT} \big|_{\frac{1}{2}^-} \simeq 0 \,. \tag{B.42}$$

Let us also consider the contribution of the Δ-resonance. For simplicity, we restrict our consideration to the leading magnetic dipole transition. The corresponding vertex can be written as [46]

$$V_{\gamma p \to \Delta}^{\alpha\mu} = \sqrt{\frac{3}{2}} \frac{(1 + m_\Delta/m)}{(1 + m_\Delta/m)^2 + 4\tau^2} \frac{G^*(Q^2)}{m^2} \varepsilon^{\alpha\mu\rho\sigma} (p_\Delta)_\rho \, p_\sigma \tag{B.43}$$

$$= V_{\gamma p \to \Delta} \left(Q^2 \right) \, \varepsilon^{\alpha\mu\rho\sigma} (p_\Delta)_\rho \, p_\sigma \,, \tag{B.44}$$

where the incoming photon momentum is defined as $q = p_\Delta - p$.

The matrix element reads, see *e.g.* [14]

$$\langle p', k' | \, O_+^\mu \, \bar{\psi} \gamma_\mu \psi \, | k, p \rangle_{\rm EFT} \big|_{\frac{3}{2}^+} \simeq G_{\rm F} \, \frac{\bar{u}' \gamma_\mu u}{q^2}$$

$$\times \int {\rm d}^D l \left[\frac{k'_\nu}{(k'l)} + \frac{k_\nu}{-(kl)} \right] \frac{1}{l^2} \left(M_{\Delta 1}^{\mu\nu} + M_{\Delta 2}^{\mu\nu} \right) \,. \tag{B.45}$$

The first contribution reads

$$M_{\Delta 1}^{\mu\nu} = \bar{N}' \left(\gamma_0 V_{p\Delta}^{\beta\nu}(l) \gamma_0 \right)^\dagger \frac{p' + l + m_\Delta}{(p'+l)^2 - m_\Delta^2} \left(-g_{\alpha\beta} + \frac{1}{3} \gamma_\beta \gamma_\alpha \right) V_{p\Delta}^{\alpha\mu}(q) N \tag{B.46}$$

$$= V_{p\Delta}(0) V_{p\Delta} \left(Q^2 \right) \frac{\varepsilon^{\alpha\mu p' p} \varepsilon^{\beta\nu p' l}}{-2(p'l) - \Delta^2} (-l^\sigma) \, \bar{N}' \gamma_\sigma \left(-g_{\alpha\beta} + \frac{1}{3} \gamma_\beta \gamma_\alpha \right) N \,, \tag{B.47}$$

where we neglected contributions with the chiral-odd structures $\bar{N}'N$, which we do not need and $\Delta^2 = m_\Delta^2 - m^2$. This expression gives the contribution, which is proportional to the following product:

$$\varepsilon^{\alpha\mu p' p} \varepsilon^{\beta\nu p' \lambda} \bar{N}' \gamma^\sigma \left(-g_{\alpha\beta} + \frac{1}{3} \gamma_\beta \gamma_\alpha \right) N \, J_{\nu\lambda\sigma} \,, \tag{B.48}$$

3-A21.30

with

$$J_{\nu\lambda\sigma} = \int dl \, \frac{1}{[l^2]} \left[\frac{k'_\nu}{(k'l)} + \frac{k_\nu}{-(kl)} \right] \frac{l_\lambda l_\sigma}{-2(p'l) - \Delta^2} \, . \tag{B.49}$$

We again use the appropriate light-cone expansions for each integral

$$l_\sigma \simeq p'_\sigma \frac{(lk)}{(p'k)} + k_\sigma \frac{(lp')}{(kp')} + l'_\top \, , \tag{B.50}$$

$$l_\sigma \simeq p'_\sigma \frac{(lk')}{(p'k')} + k'_\sigma \frac{(lp')}{(k'p')} + l_\top \, . \tag{B.51}$$

Then the contributions with p'_σ vanish due to contraction with $\bar{N}' \gamma^\sigma (\ldots) N$. Therefore, we obtain

$$J_{\nu\lambda\sigma} \simeq \int dl \, \frac{1}{[l^2]} \left[\frac{k'_\nu k'_\sigma}{(k'l)} + \frac{k_\nu k_\sigma}{-(kl)} \right] \frac{l_\lambda (lp')}{-2(p'l) - \Delta^2} \tag{B.52}$$

$$+ \int dl \, \frac{1}{[l^2]} \left[\frac{k'^\nu l'_{\top\sigma}}{(k'l)} + \frac{k_\nu l_{\top\sigma}}{-(kl)} \right] \frac{l_\lambda}{-2(p'l) - \Delta^2} \, . \tag{B.53}$$

Performing the same expansion for l_λ and taking into account rotation invariance and also using that the terms with $k_\nu k_\lambda$ and $k'_\nu k'_\lambda$ or with p'_λ vanish due to contraction with $\varepsilon^{\beta\nu p'\lambda}$ in (B.48), we find

$$J_{\nu\lambda\sigma} \sim \int dl \, \frac{1}{[l^2]} \left[k'_\nu (g_\top)'_{\sigma\lambda} \frac{l'^2_\top}{(k'l)} + k_\nu (g_\top)_{\sigma\lambda} \frac{l^2_\top}{-(kl)} \right] \frac{1}{-2(p'l) - \Delta^2} \, . \tag{B.54}$$

The UV-divergent integrals with $l'^2_\top$ and $l^2_\top$ can be understood using that

$$l^2_\top = l^2 - (p'l)(kl)\frac{1}{(p'k)} \, , \qquad l'^2_\top = l^2 - (p'l)(k'l)\frac{1}{(p'k')} \, . \tag{B.55}$$

The terms in r.h.s. of the both expressions give the scaleless integrals only and therefore also vanish. Hence, we obtain that the contribution with $M^{\mu\nu}_{\Delta 1}$ in Eq. (B.45) gives trivial contribution. The same result can be obtained in the same way for $M^{\mu\nu}_{\Delta 2}$ in Eq. (B.45). Therefore,

$$\langle p', k' | O^\mu_+ \, \bar{\psi}\gamma_\mu\psi \, | k, p \rangle_{\text{EFT}} \big|_{\frac{3}{2}+} \simeq 0 \, . \tag{B.56}$$

The similar consideration can also be used for the other resonances with $J^P = \frac{1}{2}^+, \frac{3}{2}^-$. Therefore, we conclude that we do not obtain the relevant contributions from the excited states and, therefore,

$$g_1\left(\varepsilon, Q^2\right)\big|_R = 0 \, , \qquad g_3\left(\varepsilon, Q^2\right) = 0 \, . \tag{B.57}$$

Appendix C

Estimates of the neutron FF $\mathcal{F}_{1n}$

In this section, we evaluate the FF $\mathcal{F}_{1n}$ that enters into the description of the TPE amplitudes for the neutron target. We use isotopic symmetry and known electromagnetic FFs for the proton and neutron, and proton FF $\mathcal{F}_1$ defined from the WACS data.

We start from the definition of these FFs in the EFT approach. For the hard-collinear fields, we use the same notations as in Ref. [25]. The auxiliary light-cone vectors n and $\bar{n}$ are associated with the momenta p' and p, respectively, as defined in Eqs. (B.3) and (B.4). Let us remind that we assume the Breit frame as in Ref. [25]. We also use the convenient notation for the gauge invariant combinations defined as

$$\chi_n(\lambda\bar{n}) \equiv W_n(\lambda\bar{n})\xi_n(\lambda\bar{n}) \,, \tag{C.1}$$

where the hard-collinear gluon Wilson line (WL) reads

$$W_n(z) = \mathrm{P} \exp\left\{ ig \int\limits_{-\infty}^{0} \mathrm{d}s\, \bar{n} \cdot A^{(n)}(z + s\bar{n}) \right\} \,. \tag{C.2}$$

Assuming that the nucleon electromagnetic FFs are dominated by the soft-spectator contribution in the region where the hard-collinear scale is not large $\Lambda Q < 1\ \mathrm{GeV}^2$, it is suggested that the Dirac FFs can be approximated by the corresponding matrix elements

$$F_1^p\left(Q^2\right) \simeq f_{1p}\left(Q^2\right)\,, \qquad F_1^n\left(Q^2\right) \simeq f_{1n}\left(Q^2\right)\,, \tag{C.3}$$

where the SCET FFs are defined as

$$\left\langle P\left(p'\right)\right| O_+^\mu \left|P(p)\right\rangle_{\mathrm{SCET}} = \bar{N}'\gamma_\perp^\mu N\, f_{1p}\left(Q^2\right)\,, \tag{C.4}$$

and the SCET operator reads

$$O_+^\mu = \sum_{q=u,d} e_q \left\{ \bar{\chi}_n(0)\gamma_\perp^\mu\, \chi_{\bar{n}}(0) + \bar{\chi}_{\bar{n}}(0)\gamma_\perp^\mu \chi_n(0) \right\}\,, \tag{C.5}$$

where $e_u = 2/3$ and $e_d = -1/3$. The similar definition also holds for the neutron state. The matrix element (C.4) describes the configuration with one active quark or antiquark and soft spectators, see *e.g.* Ref. [23]. The first term $\bar{\chi}_n\gamma_\perp^\mu\, \chi_{\bar{n}}$ can be associated with the active quark, the second one $\bar{\chi}_{\bar{n}}\gamma_\perp^\mu\chi_n$ with active antiquark. Therefore, we can introduce the following decomposition:

$$f_{1p} = e_u \left(f_{1p}^u - \bar{f}_{1p}^u \right) + e_d \left(f_{1p}^d - \bar{f}_{1p}^d \right)\,, \tag{C.6}$$

3-A21.32   N. Kivel

where $f_1^{u,d}$ and $\bar{f}_1^{u,d}$ describe the contributions of the quark and antiquarks, respectively. Similarly,

$$f_{1n} = e_u \left(f_{1n}^u - \bar{f}_{1n}^u \right) + e_d \left(f_{1n}^d - \bar{f}_{1n}^d \right) . \tag{C.7}$$

The isotopic symmetry implies that

$$\begin{aligned} f_{1p}^u &= f_{1n}^d \equiv f_1^u , & f_{1p}^d &= f_{1n}^u \equiv f_1^d , & \text{(C.8)} \\ \bar{f}_{1p}^u &= \bar{f}_{1n}^d \equiv \bar{f}_1^u , & \bar{f}_{1p}^d &= \bar{f}_{1n}^u \equiv \bar{f}_1^d . & \text{(C.9)} \end{aligned}$$

Let us briefly remind that these soft-overlap FFs arise in SCET with the coefficient function of the order of one in α_s. These FFs still depend on the large momentum transfer Q^2, but this behaviour is defined by the hard-collinear interactions associated with the typical scale of the order of ΛQ. Since this scale is assumed to be relatively small, we cannot develop factorisation for the SCET FFs and consider these quantities as non-pertubative.

In the asymptotic limit $Q \to \infty$, behaviour of the quark and antiquark FFs is different. The antiquarks cannot appear in the leading power contribution because the minimal Fock state is described by three quarks only. As a result, the antiquark FFs are suppressed by additional powers of $1/Q^2$. However, in the region of moderate values of the hard scale, where the hard-collinear scale is still relatively small, we suppose that the antiquark FFs are still not quite small. In what follows, we *assume* that antiquark form factors for u- and d-quarks are approximately the same

$$\bar{f}_1^u \simeq \bar{f}_1^d \equiv \bar{f}_1 . \tag{C.10}$$

Then using (C.3) and the flavor decompositions (C.6) and (C.7), we get

$$F_{1p} \simeq e_u \left(f_1^u - \bar{f}_1 \right) + e_d \left(f_1^d - \bar{f}_1 \right) = e_u f_1^u + e_d f_1^d - (e_u + e_d)\bar{f}_1 , \tag{C.11}$$

$$F_{1n} \simeq e_u \left(f_1^d - \bar{f}_1 \right) + e_d \left(f_1^u - \bar{f}_1 \right) = e_u f_1^d + e_d f_1^u - (e_u + e_d)\bar{f}_1 . \tag{C.12}$$

This can also be rewritten as

$$\begin{aligned} 2F_{1p} + F_{1n} &\equiv F_1^u = f_1^u - \bar{f}_1 , & \text{(C.13)} \\ F_{1p} + 2F_{1n} &\equiv F_1^d = f_1^d - \bar{f}_1 , & \text{(C.14)} \end{aligned}$$

where we substitute the explicit values of the quark charges. The FFs F_1^u and F_1^d are often referred to in the literature as electromagnetic FFs of u- and d-quark, respectively. Using the data for the proton and neutron FFs, these F_1^q can be easily obtained, see *e.g.* Ref. [47].

The WACS form factors are defined as [25]

$$\langle P \left(p' \right) | O_-^\mu \, | P(p) \rangle_{\text{SCET}} = \bar{N}' \gamma_\perp^\mu N \, \mathcal{F}_{1p} \left(Q^2 \right) , \tag{C.15}$$

where the SCET operator reads

$$O_-^\mu = \sum_{q=u,d} e_q^2 \left\{ \bar\chi_n(0)\gamma_\perp^\mu \chi_{\bar n}(0) - \bar\chi_{\bar n}(0)\gamma_\perp^\mu \chi_n(0) \right\} . \tag{C.16}$$

The same definition is implied for the neutron FF $\mathcal{F}_{1n}(Q^2)$, which we need to calculate. Now the antiquark components enter with the sign minus because the corresponding operator is C-even. Using the quark and antiquark FFs, we obtain

$$\mathcal{F}_{1p} \equiv \mathcal{F}_1 = e_u^2 \, f_1^u + e_d^2 f_1^d + \left(e_u^2 + e_d^2\right) \bar f_1 , \tag{C.17}$$
$$\mathcal{F}_{1n} = e_u^2 \, f_1^d + e_d^2 f_1^u + \left(e_u^2 + e_d^2\right) \bar f_1 . \tag{C.18}$$

The data for the proton WACS allows one to get information about FF $\mathcal{F}_1$ [25, 26], which can be parametrised as in Eq. (28). Then using (C.13) and (C.14), one finds

$$f_1^u = \frac{9}{10}\mathcal{F}_1 + \frac{6}{10}F_1^u - \frac{1}{10}F_1^d , \tag{C.19}$$
$$f_1^d = \frac{9}{10}\mathcal{F}_1 - \frac{4}{10}F_1^u + \frac{9}{10}F_1^d , \tag{C.20}$$
$$\bar f_1 = \frac{9}{10}\mathcal{F}_1 - \frac{4}{10}F_1^u - \frac{1}{10}F_1^d . \tag{C.21}$$

Using these relations, one finds

$$\mathcal{F}_{1n} = \mathcal{F}_1 + \frac{1}{3}\left(F_1^d - F_1^u\right) = \mathcal{F}_1 + \frac{1}{3}\left(F_{1n} - F_{1p}\right) . \tag{C.22}$$

The flavour separation has been considered in Ref. [47]. The existing data allow one to consider only two points in the $Q^2 \geq 2.5$ GeV^2 region. Using this information, we find the results for quark, antiquark, and neutron FF $\mathcal{F}_{1n}$, which are presented in Table 2.

Table 2. Results for quark and antiquark FFs, as well as for the neutron FF $\mathcal{F}_{1n}$.

Q^2, GeV^2	F_1^u	F_1^d	$\mathcal{F}_1$	f_1^u	f_1^d	$\bar f_1$	$\mathcal{F}_{1n}$
2.5	0.14	0.028	0.29	0.34	0.23	0.20	0.25
3.4	0.085	0.013	0.15	0.19	0.11	0.10	0.12

From this table, it is seen that the antiquark FF is quite large and comparable to the quark FFs f_1^q. This result is a consequence of the rather small e.m. d-quark FF: $F_1^d \ll F_1^u$. In the soft-spectator picture, this fact is naturally interpreted as a cancellation between the FF of the quark and antiquark in the region of moderate values of Q^2.

Let us remind that the antiquark FF is formally power suppressed as it follows from the naive power counting but for the soft-spectator scattering the power behaviour is associated with the hard-collinear scale, which is assumed to be relatively small. The hard coefficient functions for quark and antiquark FFs are of the order of one with respect to α_s. They have NLO corrections of the order of α_s, which have been neglected for simplicity. The hard-spectator contributions have the hard coefficient functions of the order of α_s^2 and have also been neglected.

REFERENCES

[1] M. Neubert, «Heavy-quark symmetry», *Phys. Rep.* **245**, 259 (1994), arXiv:hep-ph/9306320.

[2] C.F. Perdrisat, V. Punjabi, M. Vanderhaeghen, «Nucleon electromagnetic form factors», *Prog. Part. Nucl. Phys.* **59**, 694 (2007), arXiv:hep-ph/0612014.

[3] C.E. Carlson, M. Vanderhaeghen, «Two-Photon Physics in Hadronic Processes», *Annu. Rev. Nucl. Part. Sci.* **57**, 171 (2007), arXiv:hep-ph/0701272.

[4] J. Arrington, P.G. Blunden, W. Melnitchouk, «Review of two-photon exchange in electron scattering», *Prog. Part. Nucl. Phys.* **66**, 782 (2011), arXiv:1105.0951 [nucl-th].

[5] A. Afanasev, P.G. Blunden, D. Hasell, B.A. Raue, «Two-photon exchange in elastic electron–proton scattering», *Prog. Part. Nucl. Phys.* **95**, 245 (2017), arXiv:1703.03874 [nucl-ex].

[6] D. Borisyuk, A. Kobushkin, «Two photon exchange in elastic electron scattering off hadronic systems», *Ukr. J. Phys.* **66**, 3 (2021), arXiv:1911.10956 [hep-ph].

[7] P.G. Blunden, W. Melnitchouk, J.A. Tjon, «Two-photon exchange in elastic electron–nucleon scattering», *Phys. Rev. C* **72**, 034612 (2005), arXiv:nucl-th/0506039.

[8] S. Kondratyuk, P.G. Blunden, W. Melnitchouk, J.A. Tjon, «Delta Resonance Contribution To Two-Photon Exchange In Electron–Proton Scattering», *Phys. Rev. Lett.* **95**, 172503 (2005), arXiv:nucl-th/0506026.

[9] S. Kondratyuk, P.G. Blunden, «Contribution of spin 1/2 and 3/2 resonances to two-photon exchange effects in elastic electron–proton scattering», *Phys. Rev. C* **75**, 038201 (2007), arXiv:nucl-th/0701003.

[10] H.Q. Zhou, S.N. Yang, «*Δ*(1232) resonance contribution to two-photon exchange in electron–proton scattering revisited», *Eur. Phys. J. A* **51**, 105 (2015), `arXiv:1407.2711 [nucl-th]`.

[11] D. Borisyuk, A. Kobushkin, «Two-photon exchange in dispersion approach», *Phys. Rev. C* **78**, 025208 (2008), `arXiv:0804.4128 [nucl-th]`.

[12] D. Borisyuk, A. Kobushkin, «On *Δ* resonance contribution to two-photon exchange amplitude», *Phys. Rev. C* **86**, 055204 (2012), `arXiv:1206.0155 [hep-ph]`.

[13] D. Borisyuk, A. Kobushkin, «Two-photon exchange amplitude with πN intermediate states: Spin-1/2 and spin-3/2 channels», *Phys. Rev. C* **92**, 035204 (2015), `arXiv:1506.02682 [hep-ph]`.

[14] O. Tomalak, M. Vanderhaeghen, «Subtracted dispersion relation formalism for the two-photon exchange correction to elastic electron–proton scattering: Comparison with data», *Eur. Phys. J. A* **51**, 24 (2015), `arXiv:1408.5330 [hep-ph]`.

[15] P.G. Blunden, W. Melnitchouk, «Dispersive approach to two-photon exchange in elastic electron–proton scattering», *Phys. Rev. C* **95**, 065209 (2017), `arXiv:1703.06181 [nucl-th]`.

[16] J. Ahmed, P.G. Blunden, W. Melnitchouk, «Two-photon exchange from intermediate state resonances in elastic electron–proton scattering», *Phys. Rev. C* **102**, 045205 (2020), `arXiv:2006.12543 [nucl-th]`.

[17] J. Arrington, «Implications of the discrepancy between proton form-factor measurements», *Phys. Rev. C* **69**, 022201 (2004), `arXiv:nucl-ex/0309011`.

[18] M.E. Christy *et al.*, «Form Factors and Two-Photon Exchange in High-Energy Elastic Electron–Proton Scattering», *Phys. Rev. Lett.* **128**, 102002 (2022), `arXiv:2103.01842 [nucl-ex]`.

[19] D. Borisyuk, A. Kobushkin, «Perturbative QCD predictions for two-photon exchange», *Phys. Rev. D* **79**, 034001 (2009), `arXiv:0811.0266 [hep-ph]`.

[20] N. Kivel, M. Vanderhaeghen, «Two-Photon Exchange In Elastic Electron–Proton Scattering: QCD Factorization Approach», *Phys. Rev. Lett.* **103**, 092004 (2009), `arXiv:0905.0282 [hep-ph]`.

[21] N. Isgur, L. Smith, C.H., «Asymptotic Q^2 for Exclusive Processes in Quantum Chromodynamics», *Phys. Rev. Lett.* **52**, 1080 (1984).

[22] V.M. Braun, A. Lenz, M. Wittmann, «Nucleon form factors in QCD», *Phys. Rev. D* **73**, 094019 (2006), `arXiv:hep-ph/0604050`.

[23] N. Kivel, M. Vanderhaeghen, «Soft spectator scattering in the nucleon form factors at large Q^2 within the SCET approach», *Phys. Rev. D* **83**, 093005 (2011), `arXiv:1010.5314 [hep-ph]`.

[24] A.V. Afanasev *et al.*, «Two-photon exchange contribution to elastic electron–nucleon scattering at large momentum transfer», *Phys. Rev. D* **72**, 013008 (2005), `arXiv:hep-ph/0502013`.

[25] N. Kivel, M. Vanderhaeghen, «Two-photon exchange corrections to elastic electron–proton scattering at large momentum transfer within the SCET approach», *J. High Energy Phys.* **2013**, 029 (2013), `arXiv:1212.0683 [hep-ph]`.

[26] N. Kivel, M. Vanderhaeghen, «Wide angle Compton scattering on the proton: study of power suppressed corrections», *Eur. Phys. J. C* **75**, 483 (2015), `arXiv:1504.00991 [hep-ph]`.

[27] P.A.M. Guichon, M. Vanderhaeghen, «How to Reconcile the Rosenbluth and the Polarization Transfer Method in the Measurement of the Proton Form-Factors», *Phys. Rev. Lett.* **91**, 142303 (2003), `arXiv:hep-ph/0306007`.

[28] L.W. Mo, Y.S. Tsai, «Radiative Corrections to Elastic and Inelastic ep and up Scattering», *Rev. Mod. Phys.* **41**, 205 (1969).

[29] Jefferson Lab Hall A Collaboration (M.K. Jones *et al.*), «G_{E_p}/G_{M_p} Ratio by Polarization Transfer in $\vec{e}p \to e\vec{p}$», *Phys. Rev. Lett.* **84**, 1398 (2000).

[30] Jefferson Lab Hall A Collaboration (O. Gayou *et al.*), «Measurement of G_{E_p}/G_{M_p} in $\vec{e}p \to e\vec{p}$ to $Q^2 = 5.6$ GeV^2», *Phys. Rev. Lett.* **88**, 092301 (2002).

[31] V. Punjabi *et al.*, «Proton elastic form-factor ratios to $Q^2 = 3.5$ GeV^2 by polarization transfer», *Phys. Rev. C* **71**, 055202 (2005), `arXiv:nucl-ex/0501018`.

[32] A.J.R. Puckett *et al.*, «Recoil Polarization Measurements of the Proton Electromagnetic Form Factor Ratio to $Q^2 = 8.5$ GeV^2», *Phys. Rev. Lett.* **104**, 242301 (2010), `arXiv:1005.3419 [nucl-ex]`.

[33] J. Guttmann, N. Kivel, M. Meziane, M. Vanderhaeghen, «Determination of two-photon exchange amplitudes from elastic electron–proton scattering data», *Eur. Phys. J. A* **47**, 77 (2011), `arXiv:1012.0564 [hep-ph]`.

[34] I.V. Anikin, V.M. Braun, N. Offen, «Nucleon Form Factors and Distribution Amplitudes in QCD», *Phys. Rev. D* **88**, 114021 (2013), `arXiv:1310.1375 [hep-ph]`.

[35] V.M. Braun, A.N. Manashov, J. Rohrwild, «Baryon Operators of Higher Twist in QCD and Nucleon Distribution Amplitudes», *Nucl. Phys. B* **807**, 89 (2009), `arXiv:0806.2531 [hep-ph]`.

[36] V.L. Chernyak, A.A. Ogloblin, I.R. Zhitnitsky, «Calculation of Exclusive Processes With Baryons», *Z. Phys. C* **42**, 583 (1989) [*Yad. Fiz.* **48**, 1398 (1988)] [*Sov. J. Nucl. Phys.* **48**, 889 (1988)].

[37] I.A. Qattan *et al.*, «Precision Rosenbluth Measurement of the Proton Elastic Form Factors», *Phys. Rev. Lett.* **94**, 142301 (2005).

[38] I.A. Qattan *et al.*, «High precision measurements of the proton elastic electromagnetic form factors and their ratio at $Q^2 = 0.50$, 2.64, 3.20, and 4.10 GeV^2», `arXiv:2411.05201 [nucl-ex]`.

[39] RQCD Collaboration (G.S. Bali *et al.*), «Light-cone distribution amplitudes of octet baryons from lattice QCD», *Eur. Phys. J. A* **55**, 116 (2019), `arXiv:1903.12590 [hep-lat]`.

[40] J.Y. Kim, H.C. Kim, M.V. Polyakov, «Light-cone distribution amplitudes of the nucleon and Δ baryon», *J. Hihg Energy Phys.* **2021**, 039 (2021), `arXiv:2110.05889 [hep-ph]`.

[41] S. Riordan *et al.*, «Measurements of the Electric Form Factor of the Neutron up to $Q^2 = 3.4$ GeV^2 Using the Reaction $^3\overrightarrow{\mathrm{He}}(\vec{e}, e'n)pp$», *Phys. Rev. Lett.* **105**, 262302 (2010), `arXiv:1008.1738 [nucl-ex]`.

[42] CLAS Collaboration (J. Lachniet *et al.*), «A Precise Measurement of the Neutron Magnetic Form Factor G_M^n in the Few-GeV^2 Region», *Phys. Rev. Lett.* **102**, 192001 (2009), `arXiv:0811.1716 [nucl-ex]`.

[43] M. Beneke, V.A. Smirnov, «Asymptotic expansion of Feynman integrals near threshold», *Nucl. Phys. B* **522**, 321 (1998), `arXiv:hep-ph/9711391`.

[44] V.A. Smirnov, «Applied Asymptotic Expansions in Momenta and Masses», *Springer*, Berlin, Heidelberg 2002.

[45] R.C.E. Devenish, T.S. Eisenschitz, J.G. Korner, «Electromagnetic $N - N^*$ transition form factors», *Phys. Rev. D* **14**, 3063 (1976).

[46] H.F. Jones, M.D. Scadron, «Multipole γN–Δ form-factors and resonant photo- and electro-production», *Ann. Phys.* **81**, 1 (1973).

[47] G.D. Cates, C.W. de Jager, S. Riordan, B. Wojtsekhowski, «Flavor Decomposition of the Elastic Nucleon Electromagnetic Form Factors», *Phys. Rev. Lett.* **106**, 252003 (2011), `arXiv:1103.1808 [nucl-ex]`.

[48] L. Andivahis *et al.*, «Measurements of the electric and magnetic form factors of the proton from $Q^2 = 1.75$ to 8.83 (GeV/c^2)», *Phys. Rev. D* **50**, 5491 (1994).

[49] A.F. Sill *et al.*, «Measurements of elastic electron–proton scattering at large momentum transfer», *Phys. Rev. D* **48**, 29 (1993).